University of Denver
Digital Commons @ DU

Electronic Theses and Dissertations | Graduate Studies

1-1-2019

Development of a HEK293 Cell Line to Show Inhibition of Tau Aggregation

Justin Ray Shady
University of Denver

Follow this and additional works at: https://digitalcommons.du.edu/etd

Part of the Biochemistry Commons, and the Chemistry Commons

Recommended Citation

Shady, Justin Ray, "Development of a HEK293 Cell Line to Show Inhibition of Tau Aggregation" (2019). *Electronic Theses and Dissertations*. 1617.
https://digitalcommons.du.edu/etd/1617

This Thesis is brought to you for free and open access by the Graduate Studies at Digital Commons @ DU. It has been accepted for inclusion in Electronic Theses and Dissertations by an authorized administrator of Digital Commons @ DU. For more information, please contact jennifer.cox@du.edu,dig-commons@du.edu.

Development of a HEK293 Cell Line to Show Inhibition of Tau Aggregation

Abstract

Intracellular deposition of aggregated tau is the hallmark of several different tauopathies, the most widespread of these being Alzheimer's disease. Tau is a highly soluble, intrinsically disordered, microtubule associated protein. Tau's native function is to stabilize microtubule formation in the axons of neurons. Post translational modification such as hyperphosphorylation as well as several familial mutations allow tau to nucleate and form fibrils. These fibrils can recruit healthy monomers onto their ends in a fashion described as template-assisted growth. Tau has 6 isoforms that vary by the inclusion or exclusion of two N-terminal repeats and the inclusion or exclusion of the second of four semiconserved repeats within its microtubule binding region. Isoforms containing three repeats are described as 3R isoforms and those containing four repeats are described as 4R isoforms. In Alzheimer's disease the 3rd and 4th microtubule binding repeats form the core of fibrils within Alzheimer's disease. MAP2C is a 3R homologue of tau and MAP2D is 4R homologue and assists in microtubule stabilization. The homology of MAP2 and tau within their microtubule binding repeats gave motivation to investigate whether MAP2 could compete with tau in binding to the ends of tau fibrils and inhibit elongation. Preliminary *in-vitro* data suggest this to be the case. To further strengthen these findings, two HEK293 cell lines stably expressing two tau constructs were established; hT40P301S-EYFP, a full-length tau construct C-terminally tagged with an Enhanced Yellow Fluorescence Protein, and K18P301S-EYFP, a truncated tau construct C-terminally tagged with an Enhanced Yellow Fluorescence Protein. Monoclonal cell lines of hT40P301S-EYFP were selected and were shown to be capable of forming intracellular puncta when transfected with K18wt seeds. Monoclonal hT40P301S-YFP transfected cells were then used to show in culture inhibition of fibril formation by two truncations (tr) of MAP2, MAP2Ctr and MAP2Dtr. MAP2Ctr was able to decrease the number of cells containing puncta by 33% and MAP2Dtr showed a 54% decrease. This data further supports the findings that MAP2Ctr and MAP2Dtr are capable of inhibiting tau fibril elongation both in vitro and in culture.

Document Type

Thesis

Degree Name

M.S.

Department

Chemistry and Biochemistry

First Advisor

Martin Margittai, Ph.D.

Keywords

Aggregation, Cell culture, HEK293, Inhibition, MAP2, Microtubule Associated Protein 2, Tau

Subject Categories

Biochemistry | Biochemistry, Biophysics, and Structural Biology | Chemistry

Publication Statement

Copyright is held by the author. User is responsible for all copyright compliance.

This thesis is available at Digital Commons @ DU: https://digitalcommons.du.edu/etd/1617

Development of a HEK293 Cell Line to Show Inhibition of Tau Aggregation

_____

A Thesis

Presented to

the Faculty of Natural Sciences and Mathematics

University of Denver

_____

In Partial Fulfillment

of the Requirements for the Degree

Master of Science

_____

by

Justin R. Shady

June 2019

Advisor: Dr. Martin Margittai

©Copyright by Justin R. Shady 2019

All Rights Reserved

Author: Justin R. Shady
Title: Development of a HEK293 Cell Line to Show Inhibition of Tau Aggregation
Advisor: Dr. Martin Margittai
Degree Date: June 2019

Abstract

Intracellular deposition of aggregated tau is the hallmark of several different tauopathies, the most widespread of these being Alzheimer's disease. Tau is a highly soluble, intrinsically disordered, microtubule associated protein. Tau's native function is to stabilize microtubule formation in the axons of neurons. Post translational modification such as hyperphosphorylation as well as several familial mutations allow tau to nucleate and form fibrils. These fibrils can recruit healthy monomers onto their ends in a fashion described as template-assisted growth. Tau has 6 isoforms that vary by the inclusion or exclusion of two N-terminal repeats and the inclusion or exclusion of the second of four semiconserved repeats within its microtubule binding region. Isoforms containing three repeats are described as 3R isoforms and those containing four repeats are described as 4R isoforms. In Alzheimer's disease the 3rd and 4th microtubule binding repeats form the core of fibrils within Alzheimer's disease. MAP2C is a 3R homologue of tau and MAP2D is 4R homologue and assists in microtubule stabilization. The homology of MAP2 and tau within their microtubule binding repeats gave motivation to investigate whether MAP2 could compete with tau in binding to the ends of tau fibrils and inhibit elongation. Preliminary *in-vitro* data suggest this to be the case. To further strengthen these findings, two HEK293 cell lines stably expressing two tau constructs were established; hT40P301S-EYFP, a full-length tau construct C-terminally tagged with an Enhanced Yellow

Fluorescence Protein, and K18P301S-EYFP, a truncated tau construct C-terminally tagged with an Enhanced Yellow Fluorescence Protein. Monoclonal cell lines of hT40P301S-EYFP were selected and were shown to be capable of forming intracellular puncta when transfected with K18wt seeds. Monoclonal hT40P301S-YFP transfected cells were then used to show in culture inhibition of fibril formation by two truncations (tr) of MAP2, MAP2Ctr and MAP2Dtr. MAP2Ctr was able to decrease the number of cells containing puncta by 33% and MAP2Dtr showed a 54% decrease. This data further supports the findings that MAP2Ctr and MAP2Dtr are capable of inhibiting tau fibril elongation both *in vitro* and *in culture*.

Acknowledgements

I would firstly like to thank Dr. Martin Margittai for his mentorship and advice. Our relationship has greatly grown over the past year and I hope you know how much I appreciate your honesty, professionalism, and your brilliant mind. You helped teach me many difficult lessons about work ethic, research, and of course the field of science. I look forward to following the progression of your lab and I hope to stay in touch.

Secondly, I would like to thank my family. Specifically, I would like to thank my mother and father. Your never-ending love and support have been invaluable to me. I appreciate you both more than words can describe. You always took my calls and did your best to make sure I kept myself on track. I have no idea what, as a parent, it must be like to have a son move half way across the country. I know it has been difficult as a son to be so far away and I have nothing but gratitude for the way you have supported my dreams and decisions. I love you both dearly.

Lastly, I would like to thank my beautiful, loving, kind, fiancé. I still don't think you fully understood what you were signing up for when we started dating. From the late nights to the early mornings, from the study crams to the long weekends spent writing or grading, you have stayed by my side. You understood every inconvenience this has brought you and now you are willing to move across the country to live in my hometown. Your love and support have meant so much to me and I am lucky to have an incredible woman like you in my life.

Table of Contents

1. Chapter One: Introduction 1
   - 1.1 Alzheimer's Disease 1
   - 1.2 Microtubule Associated Protein Tau 2
   - 1.3 Microtubule Associated Protein 2 Isoforms C and D 7
   - 1.4 The Scope of My Research: In Culture MAP2 Inhibition 7

2. Chapter Two: Methods 9
   - 2.1 Tau Constructs 9
   - 2.2 MAP2 Constructs 11
   - 2.3 Plasmid Transformation 12
   - 2.4 DNA Purification 13
   - 2.5 Recombinant Protein Expression 13
   - 2.6 Protein Purification 14
   - 2.7 Protein Monomerization 16
   - 2.8 Fibril Formation 17
   - 2.9 Seeded or Templated Reaction 17
   - 2.10 HEK293 Cell Culture 18
   - 2.11 G418 Cell Death Curve 19
   - 2.12 Transfection of HEK293 Cells 21
   - 2.13 Monoclonal Selection with Flow Cytometry 22
   - 2.14 Cryopreservation of Cell Lines 24
   - 2.15 Inhibition of Aggregation in Culture 24
   - 2.16 Nuclear Staining 26
   - 2.17 Confocal Imaging 27
   - 2.18 Triton Insoluble Pelleting and Western Blot 27

3. Chapter Three: Results 30
   - 3.1 G418 Cell Death Curve 30
   - 3.2 Transfection and Selection of Stably Transfected Cell Lines 31
   - 3.3 Monoclonal Cell Line Selection by Flow Cytometry 33
   - 3.4 Transfection of Cells with K18wt Seeds to Produce Intracellular Puncta 37
   - 3.5 Inhibition of Aggregation in Culture with MAP2Ctr and MAP2Dtr 40
   - 3.6 Hoechst 34580 Staining 44
   - 3.7 Biochemical Analysis of Protein Aggregates 45

4. Chapter Four: Discussion 47
   - 4.1 Established HEK293 Cell Lines Stably Expressing hT40P301S-EYFP and K18P301S-EYFP 47
   - 4.2 Stably Transfected Cells Produce Puncta when Transfected with K18wt Seeds 49
   - 4.3 Inhibition of Intracellular Puncta Formation by MAP2Ctr and MAP2Dtr 50

4.4 Further Investigation into in-culture Inhibition Effects of MAP2Ctr and MAP2Dtr 52
4.5 Summary 53

5. References 54

6. Appendix A Construct Sequences 59

7. Appendix B Protein Purification 64

8. Appendix C MAP2 Inhibition Controls and K18P301S-YFP Puncta 66

List of Figures

Figure 1.1 Tau Isoforms. 3
Figure 1.2 Depiction of Fibril Formation. 4
Figure 1.3 Model of Tau Fibrils. 5
Figure 1.4 Template-Assisted Growth. 5
Figure 1.5 Sequence Alignment of Semi-Conserved Repeats of K18, K19, MAP2Ctr, and MAP2Dtr. 6

Figure 2.1 pET-28b Plasmid Map. 10
Figure 2.2 pcDNA3.1 Plasmid Map. 11
Figure 2.3 Concentrations of G418 for Cell Death Curve. 21
Figure 2.4 Experimental Set Up. 26

Figure 3.1 HEK293 Cells Stably Transfected with K18P301S-EYFP and hT40P301S-EYFP. 32
Figure 3.2 Flow Cytometry Data of hT40P301S-EYFP HEK293 Cells. 35
Figure 3.3 Monoclonal Cell Lines Imaged by Confocal Microscopy. 36
Figure 3.4 K18wt Seed Formation. 38
Figure 3.5 K18wt Seeded Reaction. 38
Figure 3.6 hT40P301S-EYFP Aggregates in Tau Cells and Form Puncta when Transfected with K18wt Seeds. 39
Figure 3.7 MAP2Ctr and MAP2Dtr Protein. 41
Figure 3.8 Inhibition of Aggregation by MAP2Ctr and Dtr. 42
Figure 3.9 Inhibition of hT40P301S-EYFP Aggregation with MAP2Ctr and Dtr. . 43
Figure 3.10 Tau Cells Stained with Hoechst 34580. 45
Figure 3.11 Western Blot of Supernatants of Tau Cells. 46

Abbreviations

3R	Three Repeat
4R	Four Repeat
AD	Alzheimer's Disease
Aβ	Amyloid Beta
BCA	Bicinchoninic Acid Assay
BSC-A	Back Scattering Area
CBD	Corticobasal Degeneration
CMV	Cytomegalovirus
DMSO	Dimethylsulfoxide
DNA	Deoxyribonucleic Acid
DTT	Dithiothreitol
EDTA	Ethylenediaminetetraacetic acid
EYFP	Enhanced Yellow Fluorescent Protein
FBS	Fetal Bovine Serum
FITC-A	Fluorescein Isothiocyanate Area
FSC-A	Forward Scattering Area
FSC-W	Forward Scattering Width
FTDP-17	Frontotemporal Dementia Linked to Chromosome 17
HEK293	Human Embryonic Kidney Cells
HEPES	4-(2-Hydroxyethyl)piperazine-1-ethanesulfonic acid
hT40P301S	Human Tau 40 P301S
IDP	Intrinsically Disordered Protein

IPTG	Isopropyl β-D-1-thiogalactopyranoside
K18P301S	Konstrukt 18 P301S
MAP	Microtubule Associated Protein
MEM	Minimal Essential Media
NFT	Neurofibrillary Tangles
PBS	Phosphate Buffered Saline
PHF	Paired Helical Filament
PID	Pick's Disease
PIPES	Piperazine-N,N'-bis(2-ethanesulfonic acid)
PSP	Progressive Supranuclear Palsy
RNA	Ribonucleic Acid
SD	Standard Deviation
SDS-PAGE	Sodium Dodecylsulfate Polyacrylamide Gel Electrophoresis
SEM	Standard Error of Means
TCEP	Tris(2-carboxyethyl)phosphine
TRIS	2-Amino-2-(hydroxymethyl)-1,3-propanediol
UV-Vis	Ultra Violet Visible Spectrum
EYFP	Enhanced Yellow Fluorescent Protein

1. Chapter One: Introduction

1.1 Alzheimer's Disease

Intracellular deposition of aggregated, hyperphosphorylated tau is the hallmark of multiple tauopathies, the most widespread of these being Alzheimer's Disease (AD) (1, 2). AD is pathologically characterized by the extracellular deposition of amyloid β (Aβ) as senile plaques in combination with the intracellular deposition of tau as neurofibrillary tangles. This aggregation leads to symptoms such as dementia, loss of motor function, and eventually death (3). AD is the most prevalent form of dementia and is also incurable (3). AD not only affects individuals with the disease, but also causes a great deal of suffering for the patient's loved ones and those tasked with caring for the patient. AD was responsible for the death of more than 600,000 individuals 65 and older in 2010 and is projected to take the lives of more than 1.6 million people in the year 2050 (4). The Alzheimer's Association estimates that AD cost the United States Health Care System $232 billion dollars in 2017; that number is expected to grow to more than $1.1 trillion in the year 2050 with the aging of the baby boomer population (5). There is a desperate need for further study and understanding of tau deposition, its role within Alzheimer's disease, and potential treatments to prevent tau deposition.

1.2 Microtubule Associated Protein Tau

Microtubule Associated Protein Tau, MAPT or tau, is an unstructured, highly soluble, protein whose primary role is to stabilize microtubules that assist in normal neuron function, among other physiological roles (6, 7). Tau belongs to a class of proteins described as intrinsically disordered proteins (IDP) (8–10). These proteins are characterized by low sequence complexity, low proportions of hydrophobic amino acids, and high proportions of charged and polar amino acids. IDPs lack stable secondary structures and do not take on any well-defined, globular three-dimensional structures (8). Tau stabilizes microtubule assembly by electrostatic interactions of its microtubule binding region composed of a proline rich region and 3 or 4 semiconserved microtubule binding repeats (MTBRs) with microtubules in the axon of healthy neurons (6). Although tau is classified as an IDP, it is not a random coil, and rather has a loose paperclip structure in solution that persists for brief periods of time (11, 12). There are six distinct isoforms of tau expressed in adult human neurons which are the result of alternate splicing of the MAPT gene (See Figure 1.1) (13, 14). Alternate splicing of exons 2, 3, and 10, results in the inclusion or exclusion of two N-terminal inserts, and the inclusion or exclusion of the second of four MTBRs. The longest isoform of tau is hT40 which spans 441 amino acids and has both N-terminal inserts and all four microtubule binding repeats (See Figure 1.1). The shortest isoform is hT23, it spans 352 amino acids and is missing both N-terminal inserts and the second microtubule binding repeat (15). Isoforms containing all four MTBRs are

described as four repeat isoforms (4R) and isoforms containing only three MTBRs are described as three repeat isoforms (3R). 4R and 3R isoforms are expressed at similar levels in the adult human brain (13, 16). There are two truncations of tau commonly used in research: K18 which is a 4R isoform spanning amino acids 244-372, and K19 which is a 3R isoform.

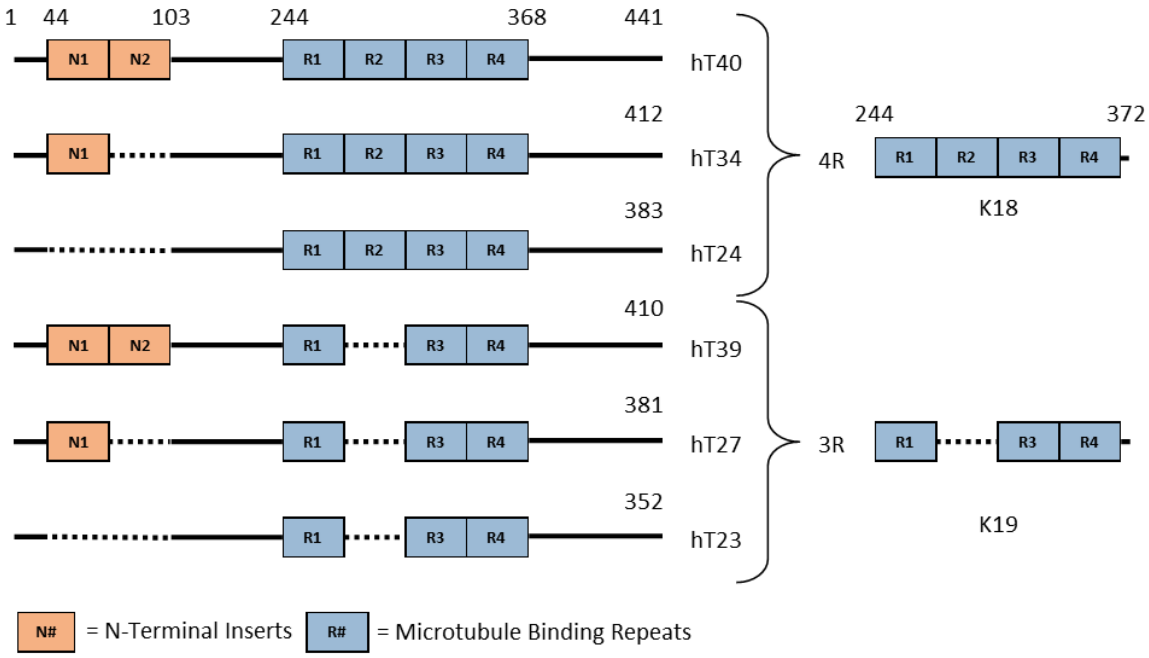

Figure 1.1 Tau Isoforms. 6 Isoforms of tau are expressed in the adult human brain. These isoforms are expressed by the alternate splicing of the MAPT gene at exons 2, 3, and 10. This results in the inclusion or exclusion of two N-terminal inserts and the second microtubule binding repeat. Two truncations commonly used in research are K18 and K19, which are composed of 4 or 3 microtubule binding repeats.

There is some evidence suggesting that post-translational modifications such as hyperphosphorylation of tau cause it to take on conformations that allow monomers to come together and nucleate (See Figure 1.2) (17–22). However, post-translational modifications are not absolutely required for aggregation to occur as recombinant, unmodified, tau is able to aggregate *in vitro* (23).

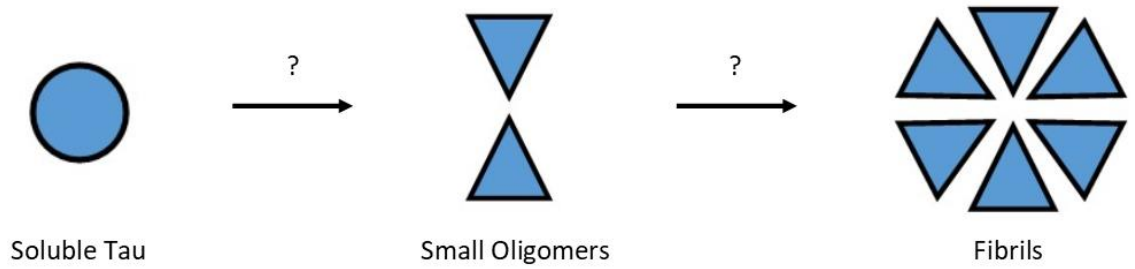

Figure 1.2 Depiction of Fibril Formation. Soluble tau undergoes a nucleation event that allows it to become amyloidogenic. It is still debated whether this nucleation event occurs with monomeric tau or whether dimers, trimers, or small oligomers. Regardless, this event leads to the formation and propagation of insoluble tau fibrils.

Upon nucleation, tau aggregates can recruit healthy soluble tau onto its ends to form fibrils. In AD, these fibrils are either paired helical filaments (PHF), or straight filaments (SF) (24, 25). The 3rd and 4th repeats of the MTBR form the core of filaments found in AD (26). Filaments are composed of structured β-sheets that stack individual strands parallel and in-register (See Figure 1.3) (27). The aggregation of tau into filaments can be facilitated by polyanions such as heparin, RNA, and arachidonic acid (28–31). In disease, aggregates are able to spread to neighboring cells where they recruit soluble tau onto their ends and create even further deposition (32–34). This method of aggregation where

monomers are recruited onto the ends of fibrils thereby assuming the same conformation as the fibril is called template-assisted growth (See Figure 1.4) (28).

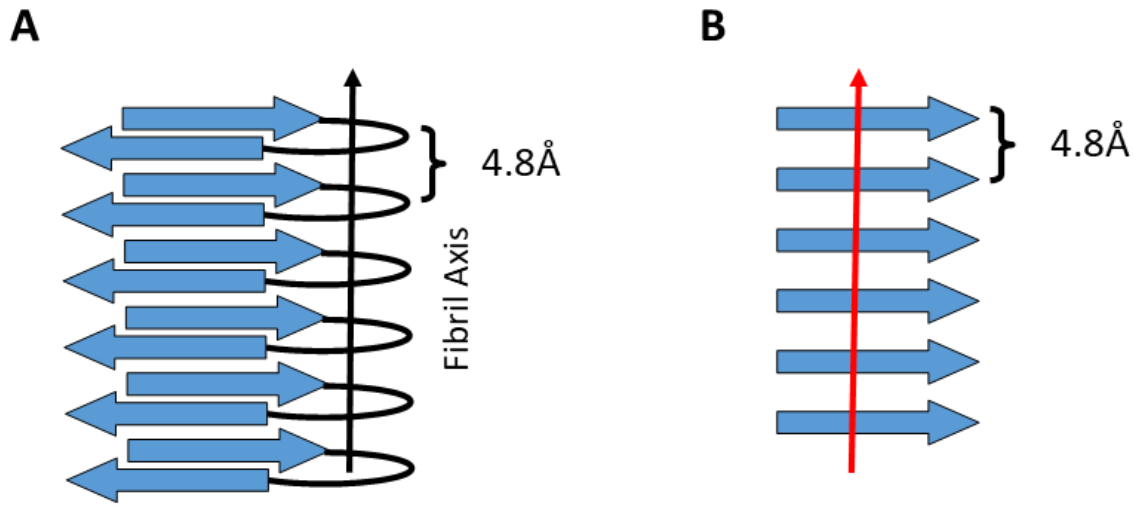

Figure 1.3 Model of Tau Fibrils. A) Stacking of monomers into β-sheets produces fibrils. B) Monomers are parrallel and in-register within the fibril. The red arrow signifying the stacking of the same amino acids ontop of one another.

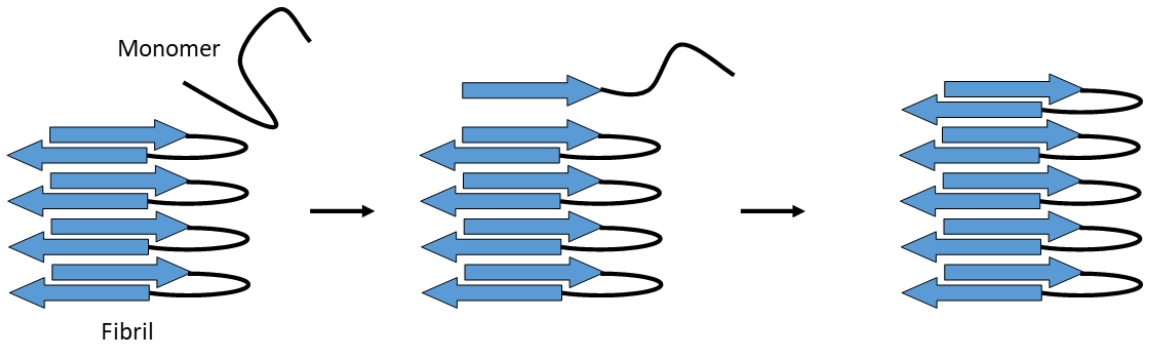

Figure 1.4 Template-Assisted Growth. Once aggregated, tau fibrils can recruit healthy monomers onto their ends. In doing so, the recruited monomer takes on the same conformation as the fibril it is growing onto. This method of recruitment is described as template-assisted growth.

Template-assisted growth offers a potential target for inhibiting fibril elongation. The ends of fibrils are responsible for the recruitment of soluble tau

and if the ends of the fibrils could be treated in a way that prevents monomer from being recruited, it could halt fibril elongation in the absence of any new breakage events (35, 36). Microtubule Associated Protein 2 (MAP2) is a homologue of tau. MAP2 stabilizes microtubule formation in a similar fashion as tau does. MAP2 has been shown to be expressed in human brains, primarily in dendrites and cell bodies (37). MAP2 and tau have high sequence homology within their MTBRs, the same sequence that forms the core of tau fibrils (See Figure 1.5). This provided motivation to investigate whether MAP2 could compete with tau to bind to the ends of fibrils and inhibit elongation.

```
K18         244 QTAPVPMPDLKNVKSKIGSTENLKHQPGGGKVQIINKKLDLSNVQSKCGSKDNIKHVPGG
K19         244 QTAPVPMPDLKNVKSKIGSTENLKHQPGGG------------------------------
MAP2Dtr     362 RLINQPLPDLKNVKSKIGSTDNIKYQPKGGQVRILNKKIDFSKVQSRCGSKDNIKHSAGG
MAP2Ctr     362 RLINQPLPDLKNVKSKIGSTDNIKYQPKGGQVQ---------------------------
                :    *:*************:*:*:** **:*:*:***:*:*:***:*********  **

K18         304 GSVQIVYKPVDLSKVTSKCGSLGNIHHKPGGGQVEVKSEKLDFKDRVQSKIGSLDNITHV
K19         304 -KVQIVYKPVDLSKVTSKCGSLGNIHHKPGGGQVEVKSEKLDFKDRVQSKIGSLDNITHV
MAP2Dtr     422 GNVQIVTKKIDLSHVTSKCGSLKNIRHRPGGGRVKIESVKLDFKEKAQAKVGSLDNAHHV
MAP2Ctr     422 ----IVTKKIDLSHVTSKCGSLKNIRHRPGGGRVKIESVKLDFKEKAQAKVGSLDNAHHV
                *.**** * :***:******** **:*:****:*:::* *****::.*:*:*****  **

K18         364 PGGGNKKIE 372
K19         364 PGGGNKKIE 372
MAP2Dtr     482 PGGGNVKID 490
MAP2Ctr     482 PGGGNVKID 490
                ***** **:
```

Figure 1.5 Sequence Alignment of Semi-Conserved Repeats of K18, K19, MAP2Ctr, and MAP2Dtr. Sequence alignment of the semi-conserved microtubule binding repeats of K18, K19, MAP2Ctr, and MAP2Dtr to show sequence homology. K18/19 are numbered with respect to hT40's sequence (Uniprot ID**:** P10636-8) and the MAP2Ctr and MAP2Dtr are numbered with respect to MAP2D's sequence (Uniprot ID: P15146-4). "*" denotes identical residues, ":" denotes conserved residues, and "." denotes semi-conserved residues. K18wt and MAP2Dtr share 66% identical, 19% conserved, and 2% semi-conserved, residues. K19 and MAP2Ctr share 65% identical, 16% conserved, and 1% semi-conserved, residues. Clustal Omega was used to align sequences.

1.3 Microtubule Associated Protein 2 Isoforms C and D

The MAP2 gene in humans encodes five different isoforms, MAP2A-D and MAP2 Isoform 3 (38). MAP2C is produced by the exclusion of exons 9, 10, 11, and 16. MAP2D is produced by the exclusion exons 9, 10, and 11, but includes exon 16 (38). MAP2D is a 4R homologue to tau and MAP2C is a 3R homologue. MAP2 is an IDP with little structure outside of its C-terminal domains, which interacts with the regulatory enzyme Protein Kinase A (38). Although MAP2 has been detected in AD brain aggregates by immunohistostaining, MAP2 has been shown to form amorphous aggregates instead of PHF under the conditions that would cause tau to aggregate (39). Preliminary work within our lab has shown that MAP2 is capable of inhibiting tau aggregation *in vitro*. In *vitro* evidence suggests that MAP2 inhibits tau elongation by competing with tau to bind onto the ends of fibrils. This data can be found in Dr. Holden's dissertation.

1.4 The Scope of My Research: In Culture MAP2 Inhibition

To strengthen these findings and increase the impact of future work, our lab saw the need to develop a cellular model of tau aggregation. Previously, other labs have used a variety of models to show intracellular tau aggregation and the inhibition thereof. Sf9 cells, insect cells isolated from *Spodoptera frugiperda*, have been used as a model for tau aggregation as tau is phosphorylated in a similar pattern to hyperphosphorylated tau in AD NFTs (40). N2a cells, mouse neuroblastoma cells, have been used to show inhibition of tau

aggregation with anthraquinones (41). Human Embryonic Kidney 293 (HEK293) cells have previously been used as a model system to investigate inhibition of tau aggregation with small peptide sequences (36). Our lab chose HEK293 as a model system to show intracellular aggregation of tau and the inhibition thereof with truncations of MAP2C and D down to residues 362-490 of MAP2D's full sequence here on referred to as MAP2Ctr and MAP2Dtr (See Figure 1.5). This cell line was selected as it is an accepted model in the field. It also has increased biological relevance as a human cell line and has been previously used to show the inhibition of tau aggregation in culture (33–36, 42–44). The use of HEK293 cells to show in the in-culture inhibition of tau aggregation by MAP2Ctr and MAP2Dtr follows.

2. Chapter Two: Methods

2.1 Tau Constructs

The longest 4R isoform of tau, hT40wt, as well as the truncated 4R tau, K18wt, were cloned into pET-28b plasmid (See Figure 2.1). This was done using the NcoI/Xho1 restriction sites (28). The synthesized DNA sequences were terminated two stop codons which prevented the transcription of the His-tag. These plasmids were then transformed into BL21 (DE3) competent cells by heat shock method for protein expression. A hT40P301S-Enhanced Yellow Fluorescent Protein (-EYFP) and a K18P301S-EYFP construct were cloned into pcDNA3.1 plasmid via HindIII/Xho1 restriction sites to be used in mammalian cell culture (See Figure 2.2). These constructs were transformed into XL1 blue cells for DNA amplification. DNA sequences can be found in Appendix A.

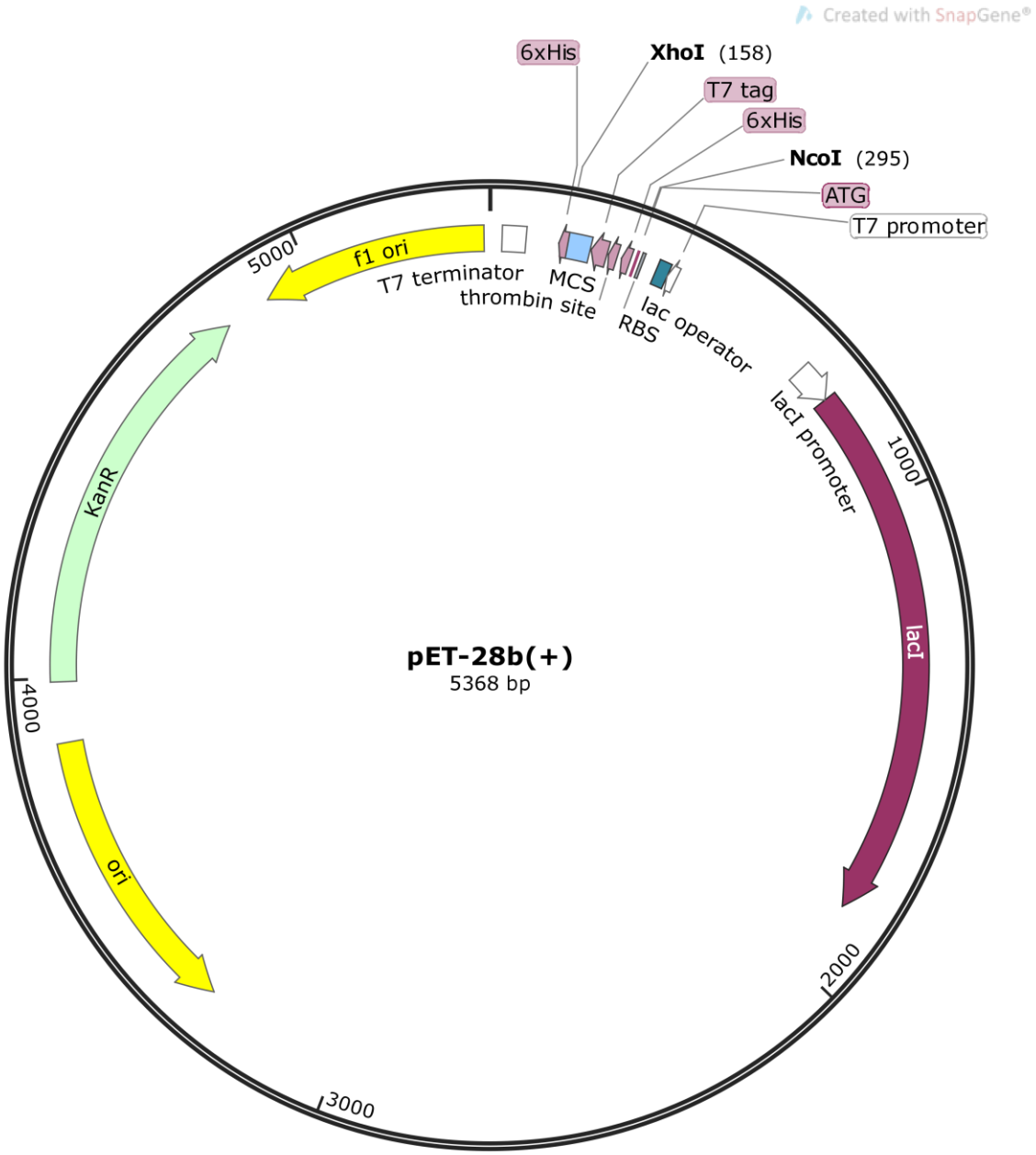

Figure 2.1 pET-28b Plasmid Map. A pET-28b plasmid map is shown above. The XhoI and NcoI restriction sites were used to clone in genes of interest. The synthesized DNA sequences were terminated with two stop codons to prevent the transcription of the 6xHis tag. The lacI gene encodes for the lac operon repressor protein that allows for induction of protein expression by IPTG. The KanR gene provides resistance to kanamycin which allows for selection of bacteria containing the plasmid. Plasmid map was created using SnapGene software (from GSL Biotech; available at snapgene.com)

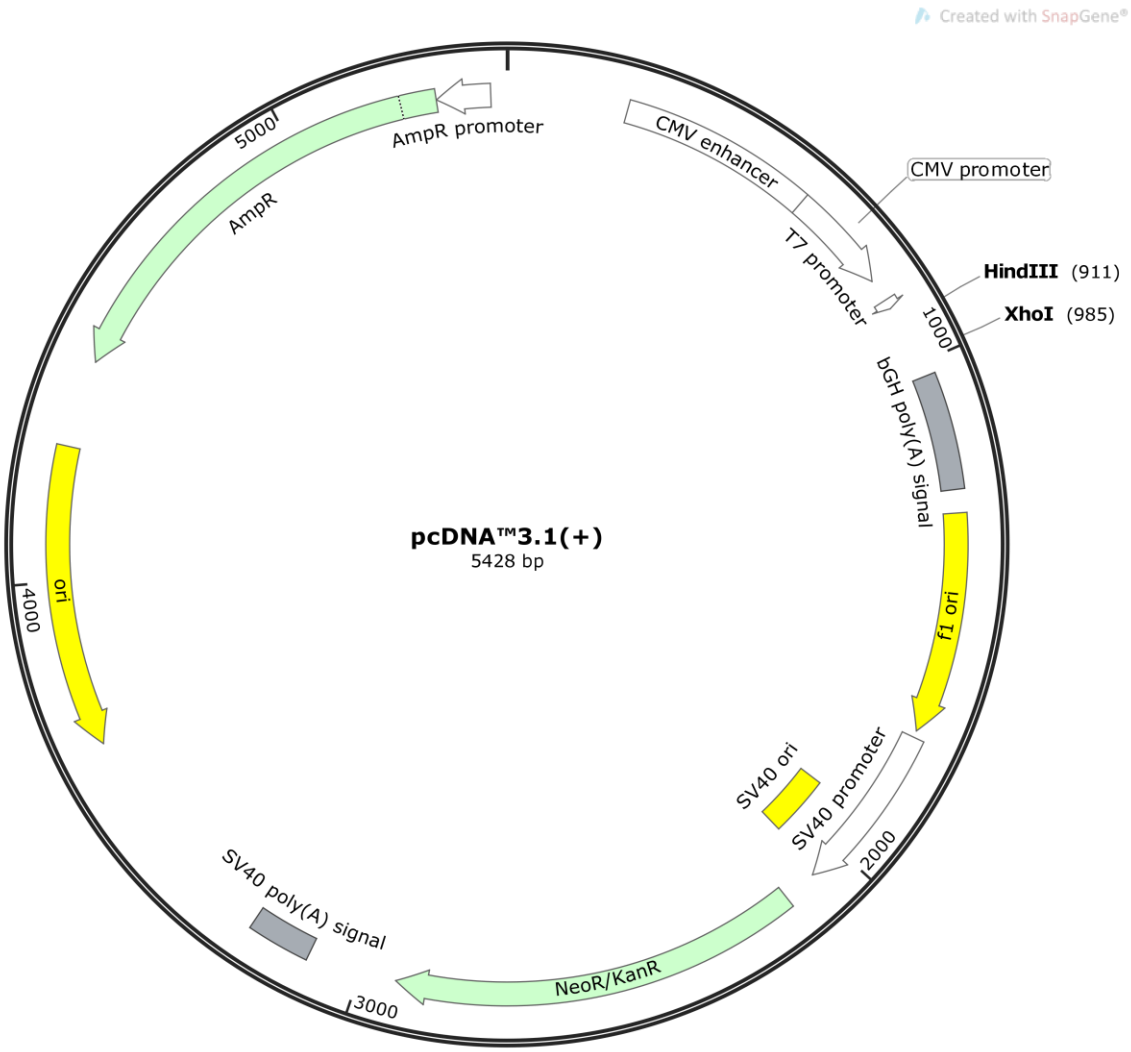

Figure 2.2 pcDNA3.1 Plasmid Map. The pcDNA3.1 Plasmid contains genes coding for ampicillin resistance which allows for the amplification of the plasmid. It also contains HindIII and XhoI restriction digest sites used to clone the genes of interest into the plasmid. Resistance to Geneticin is conferred by the NeoR/KanR gene to allow for selection of transfected cells. Plasmid map was created using SnapGene software (from GSL Biotech; available at snapgene.com)

2.2 MAP2 Constructs

MAP2C and D microtubule binding regions, MAP2Ctr and MAP2Dtr were synthesized by Biomatik. These were cloned into pET-28b plasmids using

NcoI/Xho1 restriction sites. The synthesized DNA sequences were terminated with two stop codons to prevent the transcription of the 6xHis tag. with Once cloned, the plasmids were transformed into BL21 (DE3) cells for protein expression. DNA sequences can be found in Appendix A.

2.3 Plasmid Transformation

Plasmids were transformed into either XL1 Blue Competent Cells for DNA amplification or BL21 (DE3) Competent Cells for protein expression. Cells were transformed by the following procedure. Competent cells and DNA were thawed on ice for 15 min. 30 µL of cells were pipetted into a 14 ml round bottom polypropylene tube (Corning Falcon). To this, 2 µL of pure DNA were pipetted into the cells. This mixture incubated on ice for 30 min. Following incubation, cells were heat shocked at 42 ºC for 50 seconds. At the completion of 50 seconds, the mixture was transferred back onto ice for 2 min. 800 µL of NZY+ media (10g/L NZ-amine, 12.5 mM $MgCl_2$, 12.5 mM $MgSO_4$, 20 mM glucose) was added to the cells and incubated at 37 ºC for 45 min. 50 µL of cells were plated onto LB Agar plates containing either 100 µg/mL of Ampicillin (pcDNA3.1 vector) or 50 µg/mL of Kanamycin (pET-28 vector) under sterile conditions. Plates were incubated at 37 ºC overnight until colonies grew.

2.4 DNA Purification

Plasmid DNA was transformed into XL1 Blue cells. A single colony was selected from the plate and 50 mL of autoclaved Luria-Bertani Miller broth (20 g/L, Difco) and 20 µg/mL of Kanamyacin (Gold Biotechnology) in a 125 ml Erlenmeyer flask was inoculated with the colony and incubated overnight at 37 ºC. Plasmid DNA was then purified using MIDI preparations following manufacturer's protocols (Qiagen) for pET-28 vectors. pcDNA3.1 vector was purified using E.Z.N.A. Endo-Free Plasmid DNA Midi Kits following manufacturer's protocols (Omega Bio-Tech). DNA concentrations were quantified using UV-Vis absorbance at 260 nm. Proteinaceous content, most importantly endonuclease content, was assessed by the ratio of absorbance at 260 nm and 280 nm. A ratio >1.8 of 260/280 nm was used for mammalian cell culture transfection to ensure a minimal endonuclease content.

2.5 Recombinant Protein Expression

Protocols used for protein expression are as follows. BL21 (DE3) competent cells were previously transformed with a pET-28 vector containing the sequence for the protein of interest. A 125 mL Erlenmeyer flask was filled with 50 mL of autoclaved Luria-Bertani Miller broth and 20 µg/mL of Kanamyacin. A single colony was selected off the previously prepared plate that had incubated overnight, or a prick of a previously prepared glycerol stock, and was added to the media. This was then incubated overnight at 200 RPM and 37 ºC (12-16 h) to

be used as a starter culture. 15 mL of this solution was added to each culuture flask containing 1.5 L of LB and 20 µg/mL of Kanamyacin and allowed to incubate at 200 RPM and 37 ºC until the Optical Density (OD) at 600 nm had reached 0.8-1.0. Each flask was then induced with 0.4 mM of IPTG (Gold Biotechnology) and incubated for 3.5 h. The solution was then poured into 1L Nalgene bottles and was centrifuged at 5500 x g for 10 min to pellet the cells. Pellets were resuspended in 500 mM NaCl, 20 mM piperazine-N,N'-bis(2-ethanesulfonic acid) pH 6.4 (PIPES, JT Baker), 5 mM ethylenediaminetetraacetic acid (EDTA, Fisher), and 50 mM β-mercaptoethanol (Fisher), . Resuspended pellets were transferred to 50 mL conical vials (Corning) and stored at -80 ºC.

2.6 Protein Purification

50 mL conical vials containing the resuspended pellets were thawed in an 80 ºC water bath for 20 min to precipitate any proteins that are not heat stable. Tubes were then placed on ice for 5 min and sonicated using a 6 mm tip sonicator (Fischer Scientific Model 150) at 50% power for 1 min to lyse cells and release soluble proteins. Samples were centrifuged at 20,000 g for 30 min to pellet any insoluble proteins and cellular debris. The remaining supernatant was adjusted to 55% w/v $(NH_4)_2SO_4$ (Ultra Pure, MP) and rocked for 1 h to precipitate any soluble protein. Samples were centrifuged at 4,000 x g for 10 min to pellet the precipitated protein. The supernatants were removed, and samples were centrifuged at 4,000 x g for 10 min again to remove any remaining supernatant.

Pellets were taken up in 8 mL of ultrapure water (tau) or 10 mM PIPES (pH 6.4), 150 mM NaCl, 2 M Urea (MAP Proteins), each with 4 mM dithiothreitol (DTT, Gold Biotechnology). Samples were sonicated with a 6 mm tip sonicator at 50% power for 1 min on ice to fully resuspend the pellets. Samples were syringe filtered through a 0.4 µm filter (Pall Acrodisk) to remove particulates. Samples were then diluted with the previous solutions until a conductivity below 20 mS/cm (tau) or 30 mS/cm (MAP2) was achieved. The protein sample was loaded onto a cation exchange column (Mono S 10/100 GL, GE Healthcare) with a 50 mM NaCl, 20 mM PIPES (pH 6.4), 0.5 mM EDTA, 2 mM DTT buffer. The protein was eluted using a linear gradient of 1.0 M NaCl, 20 mM PIPES (pH 6.4), 0.5 mM EDTA, and 2 mM DTT buffer. The samples were loaded onto 12% polyacrylamide gels for full length tau, or 15% polyacrylamide for truncated tau and truncated MAP2, and resolved by SDS-PAGE to select for fractions with the highest purity (Appendix B). The purest fractions were pooled and adjusted to 3 mM DTT. Fractions were stored at -80 ºC until further purification by size exclusion chromatography. The selected fractions were thawed and loaded onto a S75 size exclusion column (GE Healthcare) for truncated tau and MAP2 or a S200 size exclusion column (GE Healthcare) for full length tau. Both columns are GE Healthcare XK-26/100 columns (1000 mm height, 26 mm internal diameter). The buffer used for size exclusion was 100 mM NaCl, 20 mM 2-Amino-2-(hydroxymethyl)-1,3-propanediol (pH 7.5, TRIS, Fisher), 1 mM EDTA, and 2 mM DTT. Elution profiles can be seen in Appendix B. Collected fractions were again

run on an SDS-PAGE gel to select for the purest fractions (Appendix B). Fractions were pooled and diluted in methanol (1:1 v/v) (Fisher Optima Grade) for full length proteins or with Acetone (1:4 v/v) (Fisher Optima Grade) for truncated proteins and adjusted to 4 mM DTT in 50 mL conical vials and precipitated on ice at 4 ºC overnight. The precipitated protein was pelleted by centrifugation at 12,000 x g for 10 min. Pellets were washed twice with 100% methanol for full length protein or 100% acetone for truncated protein. Pellets were then stored under methanol or acetone adjusted to 0.5 mM Tris(2-carboxyethyl)phosphine hydrochloride (TCEP, Gold Bio) at -80 ºC.

2.7 Protein Monomerization

The supernatants were discarded from the pellets previously prepared. Pellets were resuspended in 8M Guanidinium Hydrochloride (ThermoFisher) until fully dissolved, 2-24 h. The protein solution was run over a PD-10 desalting column (GE Healthcare) that had been equilibrated using assembly buffer, 100 mM NaCl, 10 mM 4-(2-Hydroxyethyl)piperazine-1-ethanesulfonic acid pH 7.4 (HEPES, Fisher), 0.1 mM NaN_3, to exchange the protein into assembly buffer. This was done following manufacturer's protocols. Assembly buffer was also used for elution. A Bicinchoninic Acid Protein Assay (BCA, Pierce) was used following manufacturer's protocols to determine protein concentration.

2.8 Fibril Formation

To form tau aggregates, the following reaction was used. Tau concentration was adjusted to 25 µM in assembly buffer with 50 µM Heparin (Celsus, average molecular weight 4400 KDa) and 0.5 mM TCEP at a final volume of 500 µL. The reaction mixture was incubated at 37 ºC for 3 days for truncated tau and 8 days for full length tau on a Barnstead Thermolyne stir plate set to 220 RPM with a Teflon-coated micro stir bar (5x2 mm) so that the stir bar achieved 160 RPM at this setting. To assess the quality of the formed fibrils, reactions were ultra-centrifuged at 130,000 x g for 30 min in 1.5 mL ultra-centrifuge polypropylene tubes (Beckman Coulter). The supernatants (soluble fraction) and pellets (insoluble fractions) were separated and volumes were adjusted using 1 X Laemmli Sample Buffer to equivolume with respect to the original volume centrifuged. Pellets and supernatants were loaded onto 12% polyacrylamide gels for full length proteins or 15% polyacrylamide gels for truncated proteins and resolved by SDS-PAGE. The intensity of pellets and supernatants were quantified using densitometry in ImageJ (45). To assess percent growth, the following equation was used: Pellet / (Pellet + Supernatant) = % Growth.

2.9 Seeded or Templated Reaction

To assess the ability of the formed fibrils to seed monomer, the following reaction was performed. Fibrils formed in the previous step were sonicated at 2%

power for 30 seconds on ice using a Fisher Sonic Dismembrator Model 100 with a 2 mm tip to fracture the fibrils into smaller, seeding competent, fibrils. Ten µM tau and 10% monomer equivalents of seeds (1 µM Seed), 20 µM Heparin, and 0.5 mM TCEP, were incubated at 37 ºC quiescently for 12 h. The reaction was then ultra-centrifuged at 130,000 x g and pellets and supernatants were treated as described in section 2.8. The amount of protein in the pellet vs. supernatant was assessed using ImageJ densitometry measurements as described in section 2.8 (45).

2.10 HEK293 Cell Culture

HEK293 Cells were purchased from American Type Culture Collection (ATCC). Upon arrival, the cryo-frozen sample was thawed with 1 mL of 37 ºC Dulbecco's Modified Eagle Medium + GlutaMAX™-1 (DMEM, Gibco) supplemented with 10% Fetal Bovine Serum (FBS, Gibco) and 40 U/mL of Pen Strep (Gibco). 250 mL of DMEM and 27.5 mL of FBS was previously filtered through a 250 mL Rapid-Flow Filter Unit 0.45 µm Polyethersulfone membrane (Thermo) to produce 10% FBS in DMEM and to ensure sterilization. Upon thawing, 1 mL of cells were transferred into 2, 12.5 cm^2 tissue culture flasks (CELLTREAT) containing 2 mL of 10% FBS in DMEM. Cells were grown to 70% confluency with media changes every other day before being split into 8 chamber cell culture slides (8 Well Polystyrene Chamber, CELLTREAT) for transfection.

To passage cells, the media was aspirated, and cells were washed with 1 mL of Phosphate Buffered Saline (PBS pH 7.4, Gibco) to remove any dead cells and remaining media. Enough TrypLE Express Trypsin (Gibco) was added to cover the cells (~ 1 mL) to cleave integrins thus releasing the cells from the plate. The cells containing TrypLE Express Trypsin were incubated at 37 ºC for 5 min or until all cells were suspended. After that time, 1 mL of 10% FBS in DMEM was added to the cells to halt TrypLE Express Trypsin activity. The cell suspension was pipetted up and down against the bottom of the flask to break up any clumps of cells. The resulting suspension was then analyzed for cell density using a Bright Line Hemocytometer (Hausser Scientific) and plated at a density of 0.3 x 10^6 cells/well into 8 chamber cell culture slides for transfection.

2.11 G418 Cell Death Curve

G418 is isolated from living organisms and has several contaminating gentamicins other than G418 (46). This leads to discrepancies between the concentrations reported by manufacturers and the actual effective concentrations. This requires the effective concentration to be determined for each new lot of G418 and for each cell line it is used on. To determine the concentration of Geneticin (G418, Gibco) to use for selection of HEK293 cells containing the plasmid of interest, the following cell death curve was executed. HEK293 cells that had not been transfected with pcDNA3.1 plasmid were plated in triplicate wells of a 96-well plate (SensoPlate Plus Microplates F-Bottom,

Greiner Bio-One) and allowed to grow to 70% confluency in 10% FBS in DMEM with 40 U/mL of Pen Strep (Gibco). G418 was added to 10% FBS in DMEM at concentrations ranging from 400-1000 µg/mL. The 10% FBS in DMEM with Pen Strep media was aspirated off the cells and the 200 µL of 10% FBS in DMEM with G418 was added (See Figure 2.3). The media was changed every 48 h to ensure G418 concentrations were held constant and cell death was assessed visually using a Zeiss IM 35 inverted microscope. After 7 days, cell death was assessed and the concentration that had killed all cells within a well was used for transfected cell growth. This concentration was found to be 700 µg/mL of G418 and was used to select for cells containing the plasmid of interest. Once selected for, cells stably transfected with the plasmid were cultured in media containing 700 µg/mL of G418.

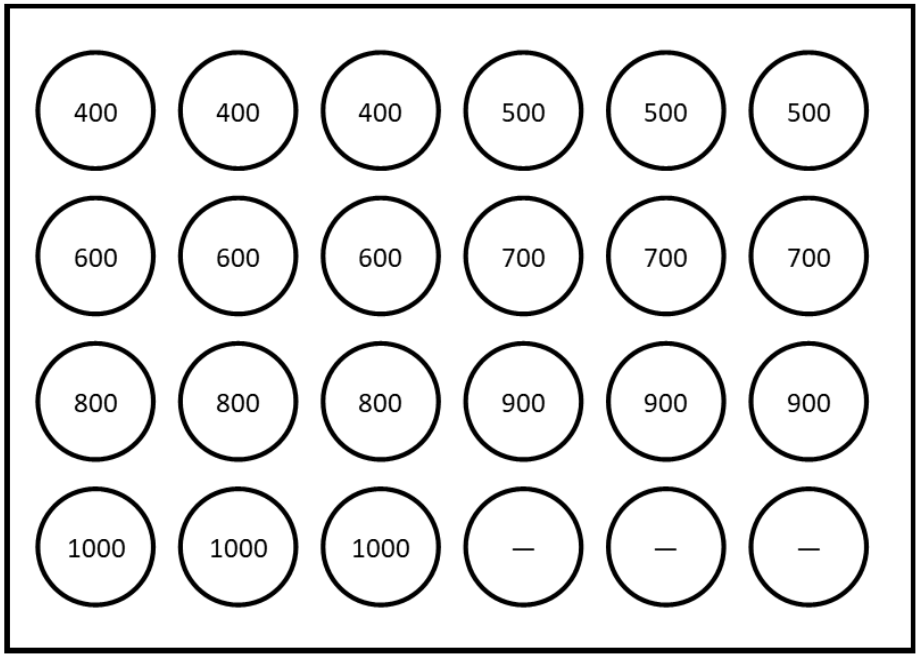

Figure 2.3 Concentrations of G418 for Cell Death Curve. Cells were incubated in DMEM containing 10% FBS and 400-1000 µg/ml of G418 in triplicate as shown above. The media was changed every 48 h to ensure concentrations of G418 stayed consistent. Cell death was assessed visually with an inverted microscope daily.

2.12 Transfection of HEK293 Cells

pcDNA3.1 plasmid containing either hT40P301S-EYFP or K18P301S-EYFP, purified previously in section 2.4, was transfected into HEK293 cells using Lipofectamine 2000 Transfection Reagent (Thermo Fisher) following manufacturer's instructions. 24 h post transfection, the media was replaced with 10% FBS in DMEM containing 700 µg/mL of G418 to select for the cells containing the plasmid of interest. After one week under selection media, cells were plated onto a 96-well plate for confocal imaging to confirm stable transfection of hT40P301S-EYFP or K18P301S-EYFP.

2.13 Monoclonal Selection with Flow Cytometry

Following one week under selection media, cells that had been stably transfected were split and re-plated into 100x20 mm culture plates (Nunc Easydish 100x20 mm, Thermo Scientific) and grown to 70% confluency. Non-transfected HEK293 cells were also plated to act as a control. Cells were then harvested using TrypLE Express Trypsin. Once cells were released from the plate, PBS containing 1% FBS was used to halt TrypLE Express Trypsin activity and the cells were transferred into a 15 mL conical vial. The cells were pelleted by centrifugation at 300 x g in a swinging bucket rotor centrifuge (IEC Clinical Centrifuge, International Equipment Company), the supernatants were removed, and the cells were washed twice with 1% FBS in PBS. Once washing was completed, cells were resuspended in 1 mL of 1% FBS in PBS and filtered through a Sterile Cell Strainer (40 µm Nylon Mesh, Fisher) to remove any clumps of cells and particulate. Cells were stored on ice until sorting. Once washed, the cells were passed through a Sony FX500 Exchangeable Fluids Cell Sorter using the following settings to achieve monoclonal cell lines. The Cell Sorter works by passing cells single file through a laser that can measure the size of cells by Forward Scattering Area (FSC-A), Back Scattering Area (BSC-A), and Forward Scattering Width (FSC-W). It can also detect the fluorescence intensity of EYFP within cells by using the Fluorescein Isothiocyanate Fluorescence Area channel (FITC-A). The program's Compensation Wizard was used to assess the control cell's FSC-A, BSC-A, and FITC-A to establish a "blank". A total of 10,000 events

were recorded. After the Compensation Wizard was completed, hT40P301S-EYFP cells were loaded into the sorter. HEK293 cells stably transfected with hT40P301S-EYFP were sorted against three gates. These gates act as a cut off for what cells pass certain set thresholds, and which that do not. Those that pass the first gate, Gate A, are then subjected to the thresholds of Gate B, and so on. First, Gate A was assigned to cells sorted with a scatter plot of FSC-A vs. BSC-A to select for cell size. Gate B sorted cells by a scatter plot of FSC-W (Forward Scattering Width) vs. FSC-A with the gate set at a 45º angle relative to the origin. This ensures a 1:1 ratio of area to width and therefore selects for single cells and not cells that may be clumped together. Gate C was to set to select for cells over a fluorescence threshold with a scatter plot of FITC-A vs. FSC-A. A 96-well plate containing 200 µL of 10% FBS in DMEM supplemented with 40 u/mL of Pen Strep per well was loaded into the sorter to be plated. The program was instructed to sort a single cell that had passed gate C into each well with a 1 s delay between wells. The plate was then incubated at 37 ºC and 5% CO_2 for one week with regular media changes until individual colonies of cells could be confirmed by using an inverted microscope. Cells were grown to 70% confluence before being split into 2 mL culture flasks. These were then allowed to grow to 70% confluence. Cells were then split into 96-well plates to confirm monoclonality by confocal microscopy with excitation at 495 nm. The remaining cells were cryo-preserved.

2.14 Cryopreservation of Cell Lines

To cryogenically preserve cells for later use, the following procedure was used. Media was aspirated off the cells and they were rinsed with 1 mL of PBS to wash away any remaining media and remove dead cells. Enough TrypLE Express Trypsin to cover the cells was added and the flask was incubated at 37 ºC for 5 min or until the cells were no longer adhered to the flask. 10% FBS in DMEM was added to halt the TrypLE Express Trypsin activity and cells were gently pipetted up and down to dissociate any clumps. The suspension was then transferred to a 15 mL conical vial and spun at 300 x g to pellet the cells. The supernatant was removed, and cells were resuspended in 1 mL of 10% FBS in DMEM to rinse the cells. The cells were pelleted again and resuspended in freezing media, (FBS supplemented with 10% v/v DMSO). The cells were then pipetted into 1.5 mL cryogenic vials (Fisher) to be frozen. Freezing must be done slowly as to not rupture the cells. This is accomplished by placing the cryo-tubes into a freezer box, and then placing the freezer box in a Styrofoam container. The container was then sealed and placed in the -80 ºC freezer for 24 hours. Once adjusted to -80 ºC, the cells were transferred to liquid nitrogen storage.

2.15 Inhibition of Aggregation in Culture

Monoclonal hT40P301S-EYFP HEK293 cells were plated at a concentration of 20,000-40,000 cells per well in a 96-well plate containing 10% FBS in DMEM supplemented with 700 µg/mL of G418. Cells adhered to the plate for 24 h.

Three-day 25 µM K18wt seeds were assessed for complete growth as described in section 2.8. Once growth was confirmed, the seeds were tip sonicated at 20% power for 30 seconds. Preincubation of seeds with or without MAP2 as well as a Buffer Control (Buffer + Heparin) and MAP2 Control (Buffer + MAP2 + Heparin) reactions were set up. Biological triplicate reactions containing 40 µM heparin and 20 µM of K18wt seeds with or without 20 µM MAP2Ctr or MAP2Dtr in assembly buffer were incubated at 37 ºC for 1 h. Controls containing 40 µM heparin in assembly buffer, and 40 µM heparin with either MAP2Ctr or MAP2Dtr were also set up and incubated. To transfect the HEK293 cells stably expressing the gene of interest, 2 µL of lipofectamine were diluted in 5 µL of OptiMem (Gibco) to which 10 µl of reaction mixture was added for a final seed concentration of 1 µM per 200 µL well. The solution was vortexed and incubated at room temp for 5 min to allow for incorporation of the proteins into the lipofectamine liposomes. This mixture was then added to each well and pipetted up and down gently to disperse (See Figure 2.4). Each reaction was performed over 3 separate wells to limit pipetting errors between wells. Cells were incubated with this mixture at 37 ºC and 5% CO_2 for 6 h. After 6 h, the media was aspirated to remove any seeds that have not been taken up by the cells and replaced with fresh media. The cells were again incubated at 37 ºC and 5% CO_2 for 6 h before they were imaged live by confocal microscopy. Cells were assessed quantitatively by number of cells with or without puncta. Cell were counted by identifying their kidney bean shaped nucleus which was void of fluorescence.

Puncta were identified as points of high fluorescent intensity within a cell, or as small, disperse, speckled, points of intensity unique from control cells. Cells that were lysed open were not counted. Unpaired t-test was performed using GraphPad Prism version 8.0.0 for Windows, GraphPad Software, San Diego, California USA, www.graphpad.com.

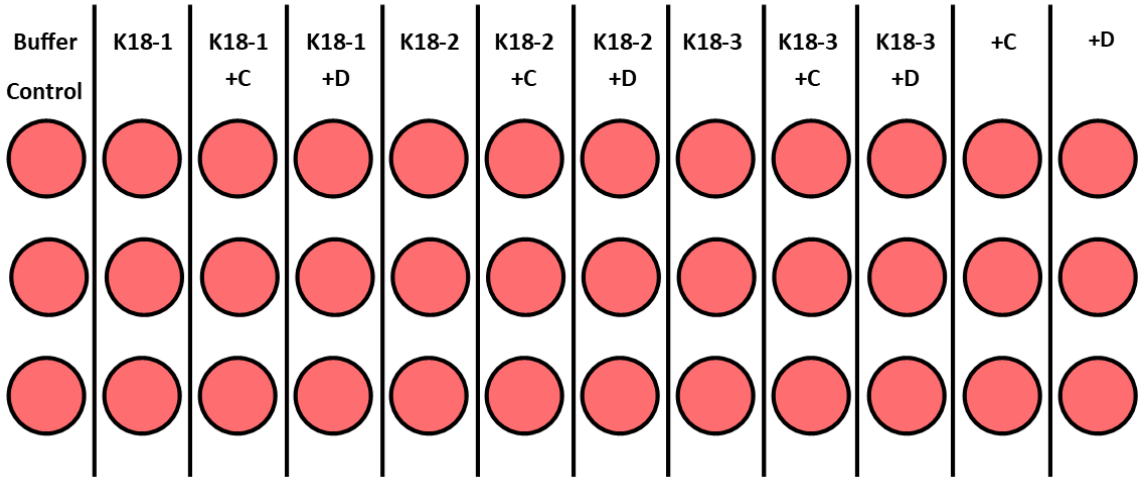

Figure 2.4 Experimental Set Up. K18-(1-3) denotes cells treated with each biological replicate of K18wt seed. +C represents cells treated with seed previously preincubated with MAP2Ctr and +D represents seed preincubated with MAP2Dtr. +C and +D are cells treated with just MAP2Ctr or MAP2Dtr without any K18wt seed. The cells treated with Buffer control contained neither K18wt seed nor MAP2.

2.16 Nuclear Staining

To better quantify cells and assess the quality of cells being imaged, Hoechst 34580 Nuclear Dye was used to stain nucleic acids within the nucleus of the HEK293 cells. To do so, the following protocol was used. Hoechst 34580 dye was diluted in ultrapure H_2O to 10 mg/mL and was tip sonicated at 20% power to fully dissolve to create a 10000X stock solution. Cells had been treated as

described in section 2.15. The Hoechst 34580 10000X stock solution was diluted to 1X in Cell Therapy Systems Dulbecco's Phosphate Buffered Saline (DPBS CTS, Gibco). 100 µL of the 1X dye was added directly to the 200 µL of media within the plate. This solution was incubated at 37 ºC for 10 min, the solution was aspirated, and replaced with 200 µL of 37 ºC 10% FBS in DMEM. The cells were then imaged via confocal microscopy.

2.17 Confocal Imaging

Cells were imaged using an Olympus IX83 Inverted Microscope in the EYFP channel using a UPlanFL N 40x/1.30 Oil objective (Olympus) or UPlanSApo 60X/1.35 Oil objective (Olympus). Laser Intensity, hv, and Gain were held constant during each individual imaging session. 3-4 images encompassing roughly 100 cells/image were taken per well for each condition. Images were uploaded to ImageJ and all intensities were normalized within the data set and analyzed for total number of cells/image, and number of cells containing puncta/image.

2.18 Triton Insoluble Pelleting and Western Blot

To further asses the inhibitory effects of MAP2Ctr and MAP2Dtr on tau aggregation in culture, the following procedure was carried out to quantify aggregation by triton insoluble pelleting followed by immunodetection via Western Blot. Following imaging, cells were harvested from the 96 well plate with

100 µL of TrypLE Express Trypsin per well. 100 µL of 1% FBS in PBS was added to each well to halt TrypLE Express Trypsin activity and cells of the same condition were pooled into 1.5 mL Eppendorf tubes. Cells were pelleted at 300 x g, the supernatants were removed, and the cells were washed with PBS to remove any remaining trypsin and re-pelleted. The supernatants were removed and 250 µL of 1% Triton Buffer containing 25 mM Tris, pH 7.5, 150 mM NaCl, 1X Halt Protease Inhibitor Cocktail (Thermo Fisher), and 1% v/v Trition X-100 (VWR International), was used to resuspend the cells. The cells were incubated on ice for 20 min and then syringe sheared through a 27 G hypodermic needle (Covidien). To ensure equal amounts of protein were loaded onto the gel, a BCA assay was performed on the total cell lysates to determine total protein concentration. To pellet insoluble proteins, 100 µL of total cell lysates were ultra-centrifuged at 130,000 x g for 30 min at 4 ºC. The supernatants were removed and enough 4X Laemmli Sample Buffer was added to achieve a 1X solution and were heated to 90 ºC. Pellets were resuspended in 1X Sample Buffer, heated to 90 ºC and tip sonicated. Samples were diluted with 1X sample buffer to match the concentration of the sample with the lowest overall protein concentration and were loaded onto 12% polyacrylamide gels and resolved with SDS-PAGE, followed by electrophoretic transfer onto PVDF Western Blotting Membrane (Sigma). All blocking, blotting, and washes were shaken on an orbital shaker during incubation periods. The membranes were blocked with 5% w/v dry milk in Tris-Buffered Saline with Tween-20 (TBST, 25 mM Tris, pH 7.5, 150 mM NaCl,

0.05% Tween-20) at 4 ºC overnight. Following blocking, the membranes were incubated for 1 h with primary antibody (GFP tag Rabbit PolyAb, #50430-2-AP Proteintech) diluted in 5% w/v dry milk in TBST at 4 ºC. The primary antibody solution was removed, and the membrane was washed 5x for 5 min with 5 mL of 5% w/v dry milk in TBST. After washing, the membranes were incubated with secondary antibody (Peroxidase-conjugated Anti-Rabbit Goat, #SA00001-2 Proteintech) diluted in 5% w/v dry milk in TBST at 4 ºC for 1 h. The secondary antibody solution was removed, and the membrane was washed 5x for 5 min with 5 mL of 5% w/v dry milk in TBST. A final wash with 5 mL Tris-buffered saline without Tween-20 was performed for 5 min. Following washing the, immunoreactivity was detected using SuperSignal West Femto Maximum Sensitivity Substrate (Thermo Scientific). Densitometry was then determined via ImageJ to quantify the signal of the resulting bands. The amount of EYFP labeled tau in pellets was compared.

3. Chapter Three: Results

3.1 G418 Cell Death Curve

Our lab saw the need to establish a cell line that could act as a model system for the in-culture aggregation of tau to further strengthen our *in vitro* findings that MAP2Ctr and MAP2Dtr are capable of inhibiting tau aggregation. The cell line HEK293 was chosen as it is a human cell line that has been previously used to investigate the in-culture aggregation of tau and the inhibition there of. Upon receiving the cells, they had to first be transfected with the plasmid containing the gene of interest. Once transfected, the cells that were stably transfected had to be selected for. The pcDNA3.2 plasmid contains a neomycin resistance gene that allows for the selection of stably transfected cells with G418. G418 is isolated from *Micromonospora rhodorangea* and the reported concentrations vary, and some cell lines are more sensitive to the antibiotic than others. This necessitates the establishment of a G418 cell death curve to determine a working concentration of G418. Upon completion of the 7-day cell death curve, it was found that 700 µg/mL of G418 in 10% FBS in DMEM was an effective working concentration. Now that this had been established, cells could be transfected with the gene of interest and those that were stably transfected could be selected for.

3.2 Transfection and Selection of Stably Transfected Cell Lines

HEK293 cells were transfected with either hT40P301S-EYFP or K18P301S-EYFP. The P301S mutation, a familial mutation found in FTDP-17, was used because other groups have previously shown that hT40 wild type (wt) does not aggregate when seeded within this system (47). The -EYFP tag allows for the detection of tau via confocal microscopy and the detection of aggregate formation by grouping of the -EYFP into puncta. Twenty-four h after transfection the cells were subjected to selection media containing 700 µg/mL of G418. After 7 days of incubation, cells were plated onto 96-well plates for imaging to confirm stable transfection of the construct. In Figure 3.1 one can see the stable transfection of both constructs within HEK293 cells.

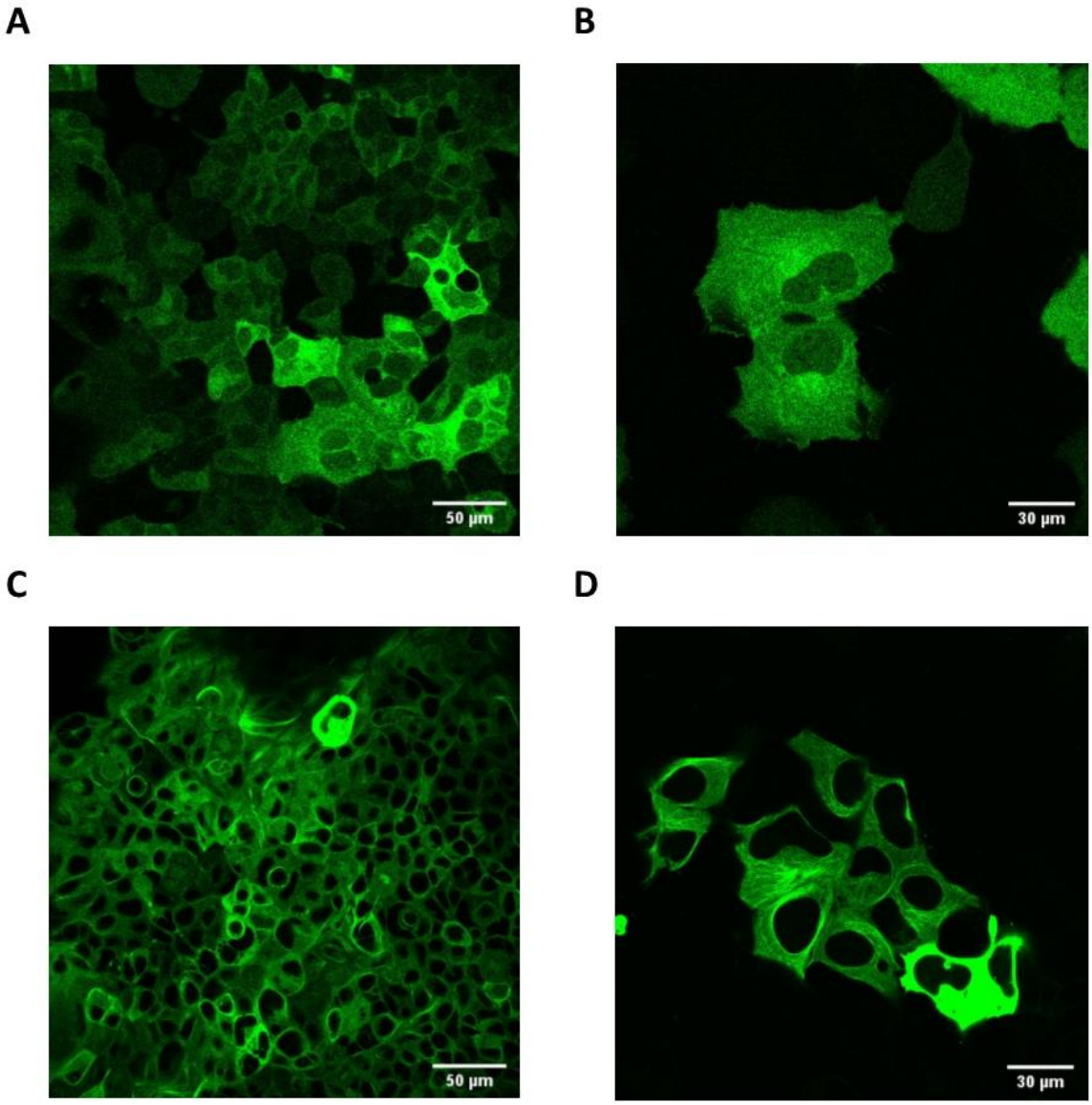

Figure 3.1 HEK293 Cells Stably Transfected with K18P301S-EYFP and hT40P301S-EYFP. A & B) HEK293 cells stably transfected with K18P301S-EYFP imaged in the EYFP channel. K18P301S-EYFP can be seen expressing diffusely throughout the cell. Different cells can be seen expressing different levels of the protein C & D) HEK293 cells stably transfected with hT40P301S-EYFP imaged in the EYFP channel. The EYFP fluorescence outlines a web-like structure that may suggest interaction of the hT40P301S-EYFP with the microtubule network of the cell. The construct is expressing at varying levels in different cells and is absent in the nucleus. Scale bars in A and C are 50 µm. Scale bars in B and D are 30 µm. A and C were imaged with a 40X UPlanFL N oil objective. B and D were imaged with a 60X UPlanSApo oil objective.

The cells are stably expressing the EYFP-tagged tau constructs. In the K18P301S-EYFP cells, the EYFP can be seen diffuse throughout the cell with small amounts fluorescing within the nucleus. In contrast, within the hT40P301S-EYFP cell the EYFP seems to colocalize with microtubules as web like structure can be observed and their nucleus is devoid of fluorescence. No puncta are observed which suggests the tau constructs are soluble and not aggregated. These stably transfected cells, however, are expressing the EYFP tagged constructs at varying levels between cells. This leads to complications with imaging where some cells are too dim to be observed (low expression levels) or too intense and saturate the camera (high expression levels) within the same field of view. To overcome this, monoclonal selection was performed to produce cells that express the EYFP-tagged constructs at uniform levels.

3.3 Monoclonal Cell Line Selection by Flow Cytometry

To achieve even fluorescent intensity across all cells in the plane of view, cells that had been previously stably transfected with hT40P301S-EYFP were sorted using a Sony FX500 Exchangeable Fluids Cell Sorter to select for a monoclonal cell line that will express our constructs at the same level. Cells that passed the gating described in section 2.13 were collected in a 96-well plate containing 200 µl of DMEM with 10% FBS and 80 U/ml of Pen Strep. In all, 10,000 total cells were counted with 87.71% passing gate A, 44.11% passing gate B, and 31.84% passing gate C (See Figure 3.2). Cells that passed gate C

were plated at a concentration of 1 cell/well. Once these cells had grown to confluency, they were imaged by confocal microscopy to ensure they had even fluorescence intensity and to select a cell line for further experiments (See Figure 3.3).

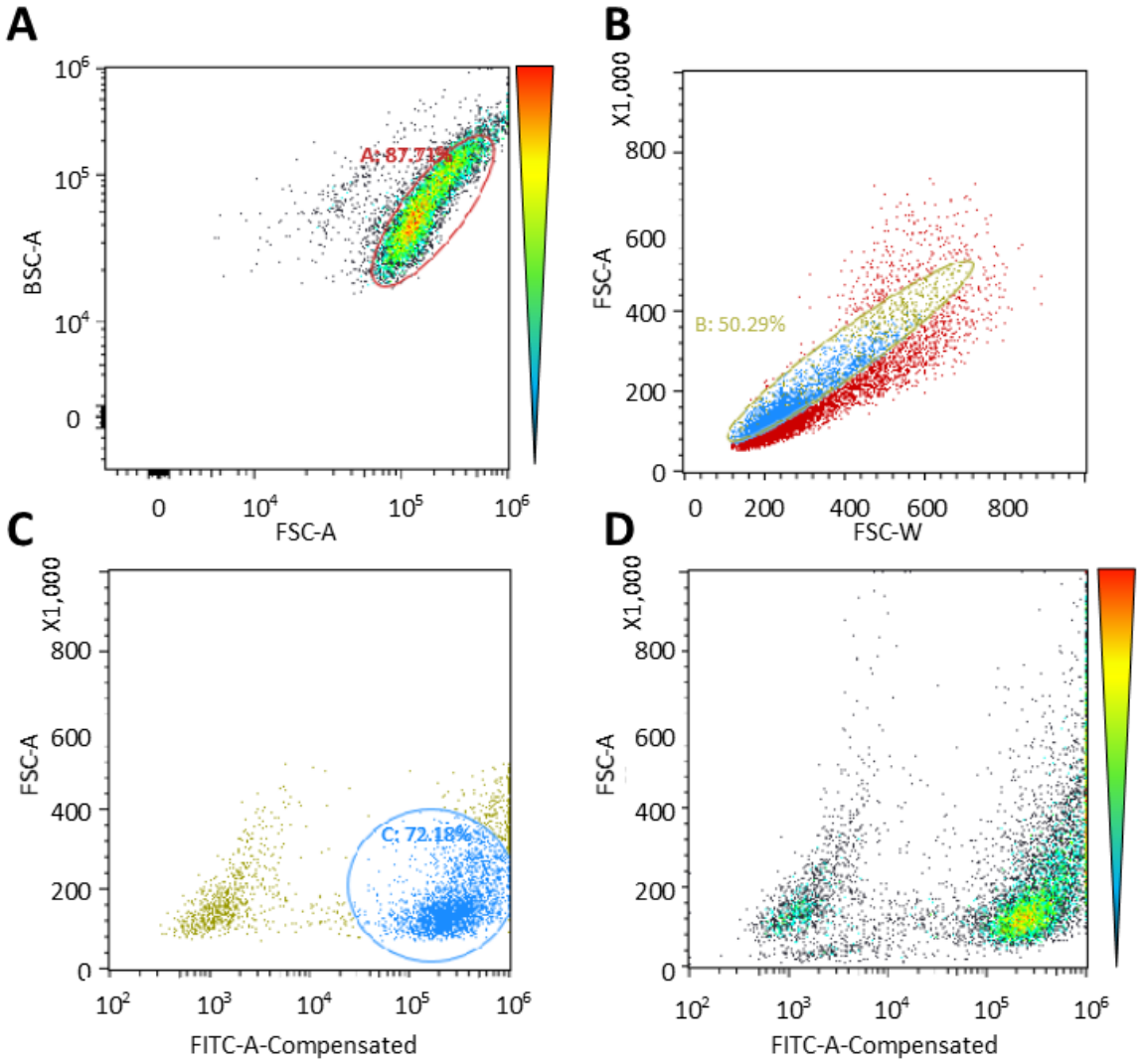

Figure 3.2 Flow Cytometry Data of hT40P301S-EYFP HEK293 Cells. Cells were gated first by FSC-A vs BSC-A (A), then by FSC-W vs. FSC-A (B), and finally by FSC-A vs FITC-A-Compensated (C). Cells that passed gate C were selected and plated at a concentration of 1 cell/well. D) Shows the distribution of cells that passed through gate B. The lower intensity cells around 10^2 FITC-A are possibly in G-Phase and not expressing as much protein resulting in lower fluorescence. Red in the heat bars of A and D represent a higher cell count whereas black represents a lower cell count. Blue dots that are circled in B and C represent cells that passed the gating.

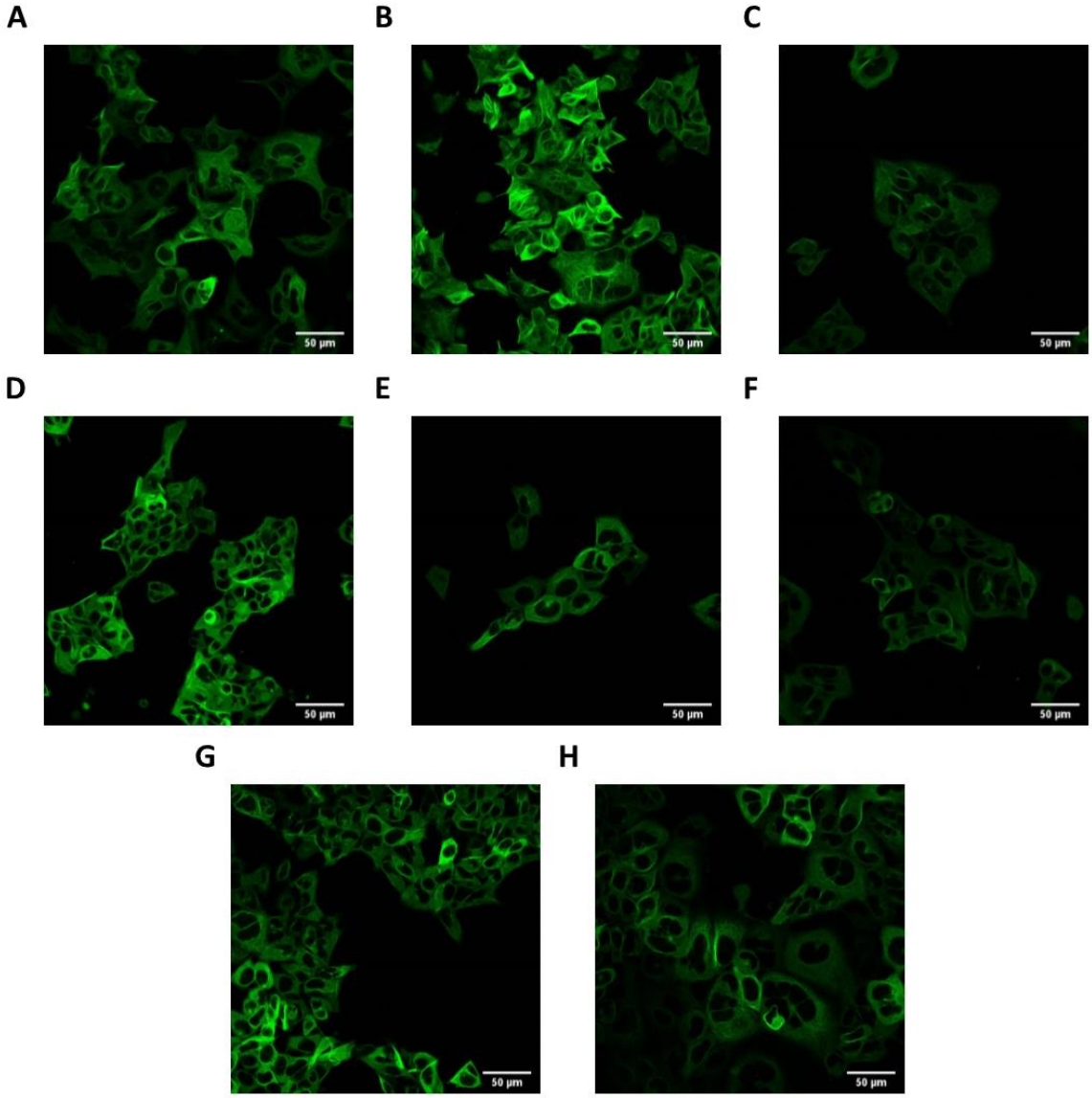

Figure 3.3 Monoclonal Cell Lines Imaged by Confocal Microscopy. A-H show various monoclonal cell lines selected for by flow cytometry. They show uniform fluorescence intensity and contain no puncta. Brightness was adjusted to be uniform in all images. The cells shown in panel D were used for further experiments. All scale bars are 50 µm. All images were viewed with a 40X UPlanFL N oil objective.

The cells in panel D of Figure 3.3 are monoclonal and stably expressing hT40P301S-EYFP. From here on out they are referred to as Tau Cells. All other monoclonal cell lines were cryopreserved. Now that a monoclonal cell line has

been established, it was necessary to show that the hT40P301S-EYFP within Tau Cells can be recruited by transfected K18wt seeds to form intracellular puncta.

3.4 Transfection of Cells with K18wt Seeds to Produce Intracellular Puncta

Before cells could be transfected with K18wt seeds, it was necessary to show that the fibrils were fully formed and that after sonication they were seeding competent. To do so, fibrils were sedimented as described in Section 2.8, and an overnight seeded reaction of K18wt monomer and K18wt seeds was performed as described in section 2.9 (See Figure 3.4 and Figure 3.5). Fibrils were found to be fully grown and could seed monomeric K18wt into fibrils. Cells were transfected with 1 µM K18wt seeds that had been tip sonicated for 30 seconds. After 12 h of incubation with seeds, the cells were imaged. Control cells showed no intracellular puncta and hT40P301S-EYFP stayed diffuse throughout the cell. Cells that had been transfected with seeds showed intracellular puncta formation after 12 h with close to 40% of cells containing puncta. The data indicates that the hT40P301S-EYFP within Tau Cells can form distinct intracellular puncta when transfected with K18wt seeds (See Figure 3.6). We next sought to determine if a decrease in the number of cells containing puncta could be observed when seeds were preincubated with MAP2Ctr and MAP2Dtr prior to being transfected into Tau Cells.

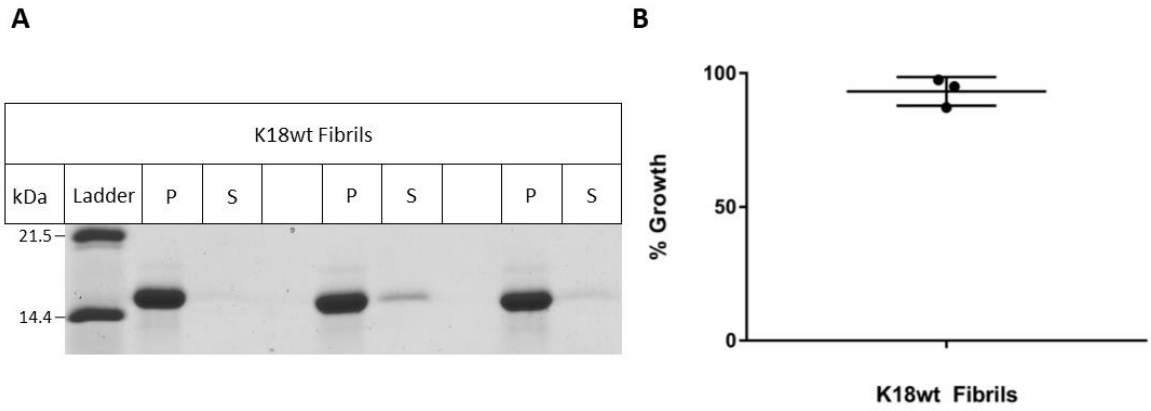

Figure 3.4 K18wt Seed Formation. A) Triplicates of 3-day K18wt fibrils were pelleted by ultra-centrifugation. Pellets (P) and supernatants (S) were loaded onto a 15% polyacrylamide gel and resolved by SDS-PAGE and stained with Coomassie stain. B) Densitometry measurements were made using ImageJ software and processed using Graph Pad Prism. Percent growth was quantified by the equation P/(P+S). The bars in B depict the mean and standard deviation of the triplicates.

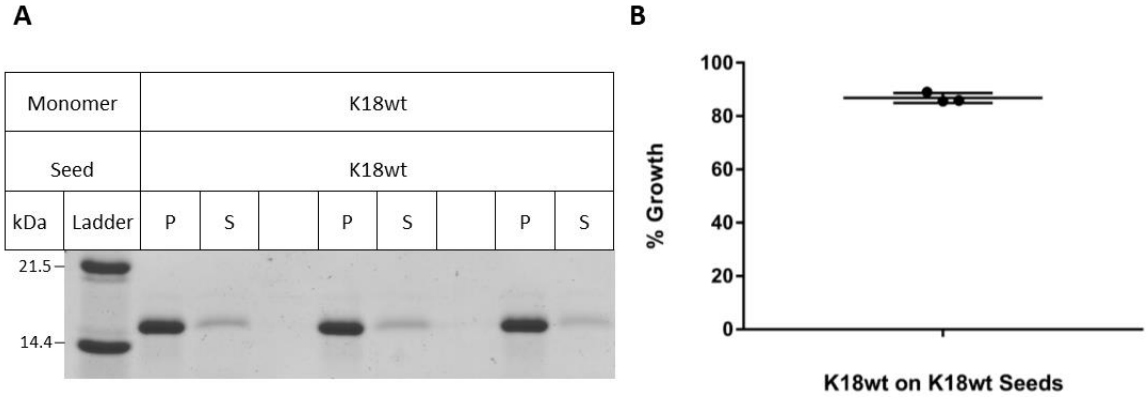

Figure 3.5 K18wt Seeded Reaction. K18wt monomer was grown onto 10% seed:monomer 3-day K18wt seeds, quantified in Fig. 3.4, overnight. A) These reactions were pelleted by ultra-centrifugation. Pellets (P) and supernatants (S) were loaded onto a 15% polyacrylamide gel and resolved by SDS-PAGE and stained with Coomassie stain. B) Densitometry measurements were made using ImageJ software and processed using Graph Pad Prism. Percent growth was quantified by the equation P/(P+S). The bars in B depict the mean and standard deviation of the triplicates.

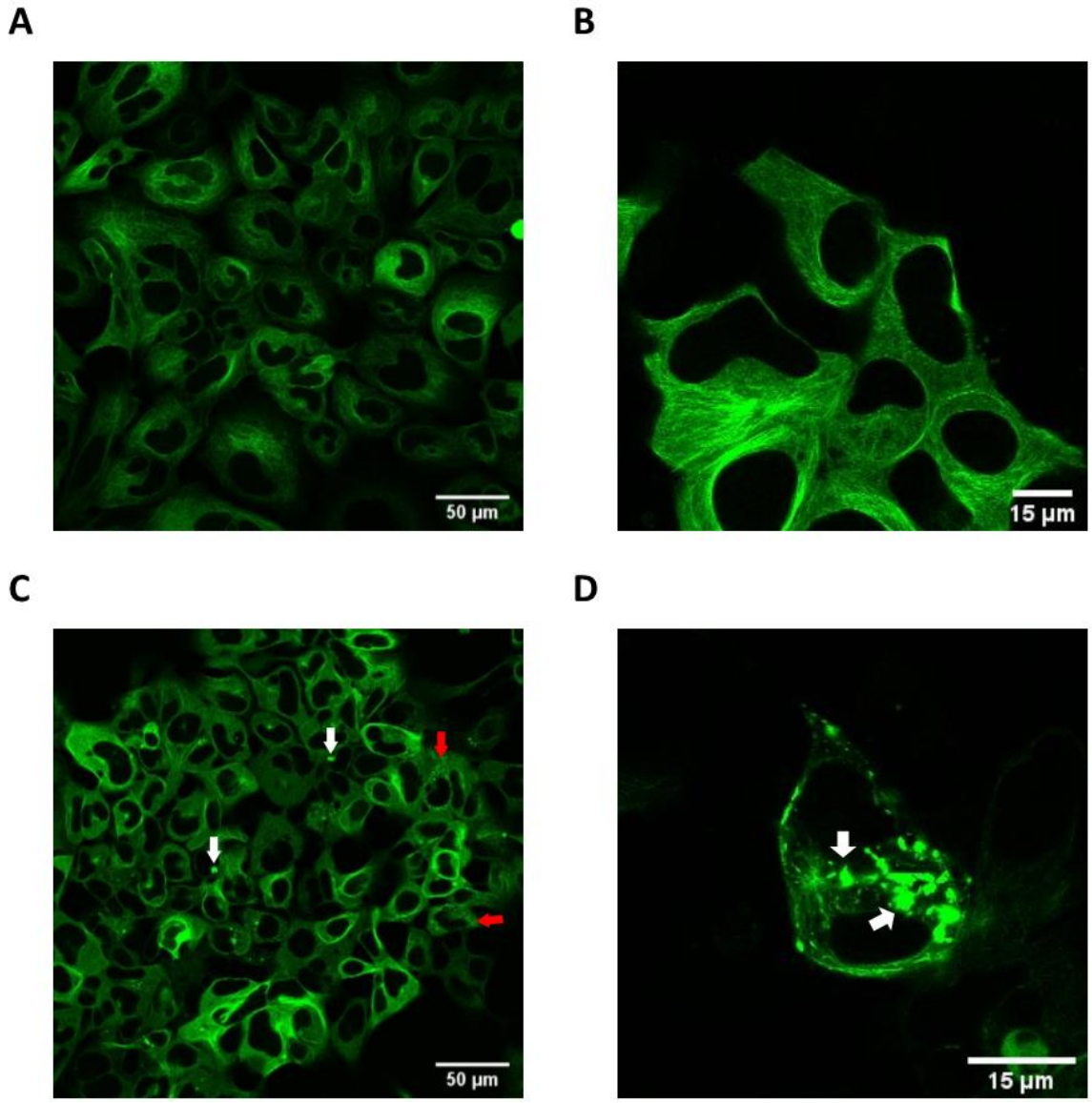

Figure 3.6 hT40P301S-EYFP Aggregates in Tau Cells and Form Puncta when Transfected with K18wt Seeds. A & B) Tau Cells transfected with a buffer control and incubated for 12 h. After incubation, the hT40P301S-EYFP stays diffuse throughout the cell with no visible puncta formation. C & D) Tau Cells transfected with K18wt seeds and incubated for 12 h. After incubation, distinct intracellular puncta can be observed. Scale bars in A and C are 50 µm and the scale bars in B and D are 15 µm. The white arrows in panels C and D denote large intercellular puncta. The red arrows denote speckled intercellular puncta. A, B, and C were all imaged with a 40X UPlanFL N oil objective. D was imaged with a 60X UPlanSApo oil objective.

3.5 Inhibition of Aggregation in Culture with MAP2Ctr and MAP2Dtr

Tau Cells have been shown to form intracellular puncta when transfected with K18wt seeds. We now sought to determine whether puncta formation could be inhibited by pretreating the K18wt seeds with MAP2Ctr or MAP2Dtr. MAP2Ctr and MAP2Dtr can be seen resolved by SDS-PAGE and stained with Coomassie stain in Figure 3.7. Tau Cells were transfected with either 1 µM K18wt seeds, 1 µM K18wt seeds preincubated with 1 µM MAP2Ctr, or 1 µM K18wt seeds preincubated with 1 µM MAP2Dtr. This was done with three separate sets of K18wt seeds to form biological triplicates. Tau Cells were also transfected with buffer alone, MAP2Ctr alone, and MAP2Dtr alone, to act as controls to show that MAP2Ctr and MAP2Dtr do not form puncta. After 6 h of incubation with seeds, the media was changed to remove any seeds that had not been taken up by the cells and cells were incubated for an additional 6 h. After this time, cells were imaged and the number of cells containing puncta vs the total number of cells were quantified. Images were collected from three separate wells of each condition. Over 1000 cells per condition were counted. A significant decrease in the number of cells containing puncta was observed when K18wt seeds were preincubation with MAP2Ctr and MAP2Dtr compared to cells that received K18wt seeds that had not been preincubated with MAP2. Cells given K18wt seeds saw 38.5 +/- 1.2% of cells containing puncta, alternatively, cells given seeds preincubated with MAP2Ctr saw only 26.8 +/- 0.2% of cells containing puncta and only 18.3 +/- 3.0% for seeds preincubated with MAP2Dtr. When normalized

so that the number of cells containing puncta when transfected with K18wt seeds alone is equal to 100%, this represents a 32.9% decrease in cells with puncta for MAP2Ctr and a 54.3% decrease in cells with puncta for MAP2Dtr (See Figure 3.8 and Figure 3.9). Tau Cells given buffer alone with no seed, MAP2Ctr, or MAP2Dtr, showed no puncta formation (See Appendix C). Collectively, the data revealed that MAP2Ctr and MAP2Dtr are capable of inhibiting tau fibril elongation in culture. Total cell count was determined by counting the dark spaces where the nucleus is. To reassure ourselves that the cell count was accurate, we sought to use a nuclear dye that would assist in differentiating individual cells from one another.

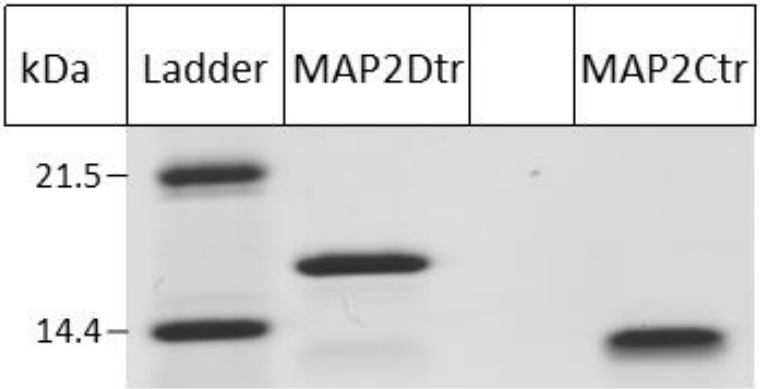

Figure 3.7 MAP2Ctr and MAP2Dtr Protein. 10 µM MAP2Ctr and MAP2Dtr loaded onto a 15% polyacrylamide gel and resolved by SDS-PAGE to show protein purity.

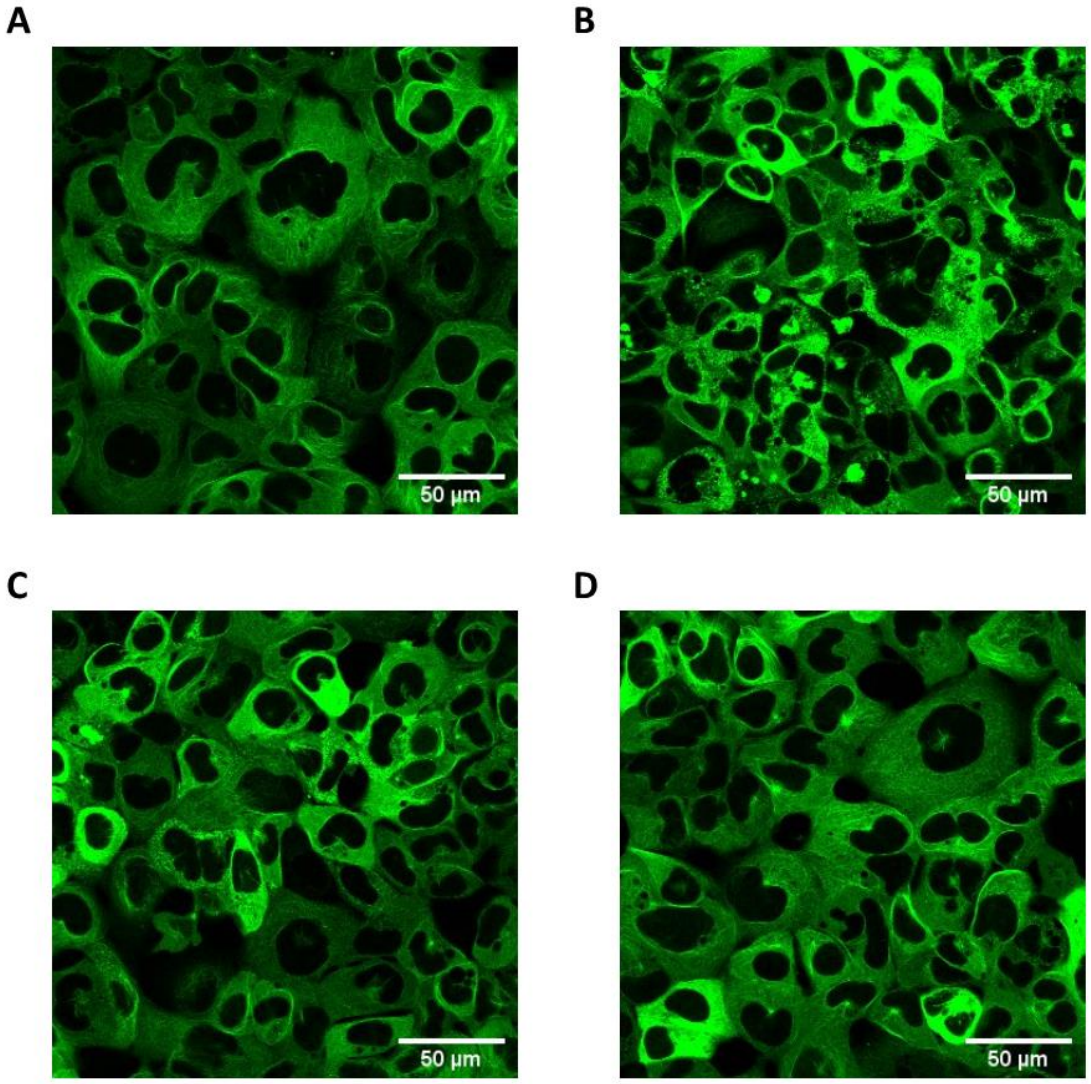

Figure 3.8 Inhibition of Aggregation by MAP2Ctr and Dtr. A) Tau Cells transfected with a buffer control. Tau is diffuse throughout the cell and void from the nucleus. B) Tau Cells transfected with K18wt seeds. Aggregated hT40P301S-EYFP are observable as distinct puncta, 38.5% of cells contain puncta. C) A 33% normalized reduction in cells containing puncta was observed in Tau Cells that were given K18wt preincubated with MAP2Ctr. D) A 54% normalized reduction in Tau Cells containing puncta was observed when K18wt seeds were preincubated with MAP2Dtr. All scale bars are 50 µm. Brightness was adjusted to be consistent in all images. All images were viewed with a 40X UPlanFL N oil objective

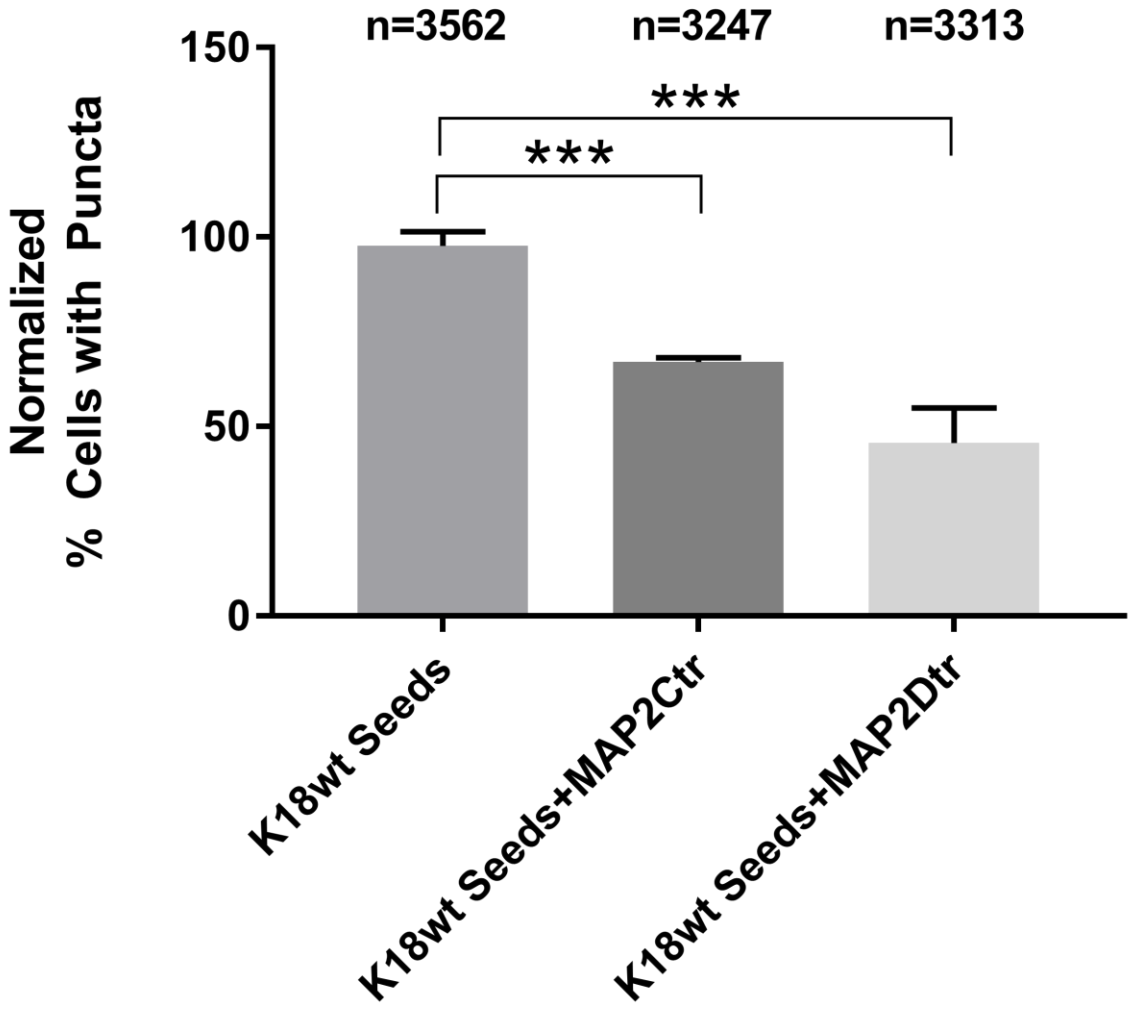

Figure 3.9 Inhibition of hT40P301S-EYFP Aggregation with MAP2Ctr and Dtr. Tau Cells were separately transfected with biological triplicates of K18wt seed that had either been untreated or preincubated with either MAP2Ctr or MAP2Dtr. Percent total cells containing puncta were quantified after 12 h of incubation with these seeds. Data was normalized to K18wt without MAP2 preincubation. The bars represent the mean of biological triplicates with error bars representing SD. Statistical significance was assessed by unpaired t-test via Graph Pad Prism. ***=$p \leq 0.001$. This decrease in the number of cells containing puncta when K18wt is preincubated with either MAP2Ctr or MAP2Dtr suggests that MAP2Ctr and MAP2Dtr are capable of inhibiting K18wt's ability to recruit soluble tau in culture.

3.6 Hoechst 34580 Staining

Previously, total cell count was assessed visually by counting the nuclei which were assumed to be the dark spots devoid of EYFP fluorescence in the center of cells. However, some cells under stressed conditions had nuclei that had divided, thus making counting difficult. Without a stain the nuclei could not be confirmed. To improve upon this method of counting, Hoechst 34580 nuclear stain was applied to the cells. Hoechst 34580 was chosen because it is cell-permeant and can be used to image live cells without the need to fix or permeate the membrane. Hoechst fluoresces upon binding to double stranded DNA and has a very small background signal. Preliminary data of the nuclear staining can be seen in Figure 3.10. Unfortunately, current staining protocols result in a significant number of cells being washed away and the appearance of the cells changes following treatment. Cells have been observed rounding up and their fluorescence intensity increases after treatment. Changes to the protocol will continue to be assessed. To further support the confocal findings, triton insoluble pelleting of in culture aggregates was used.

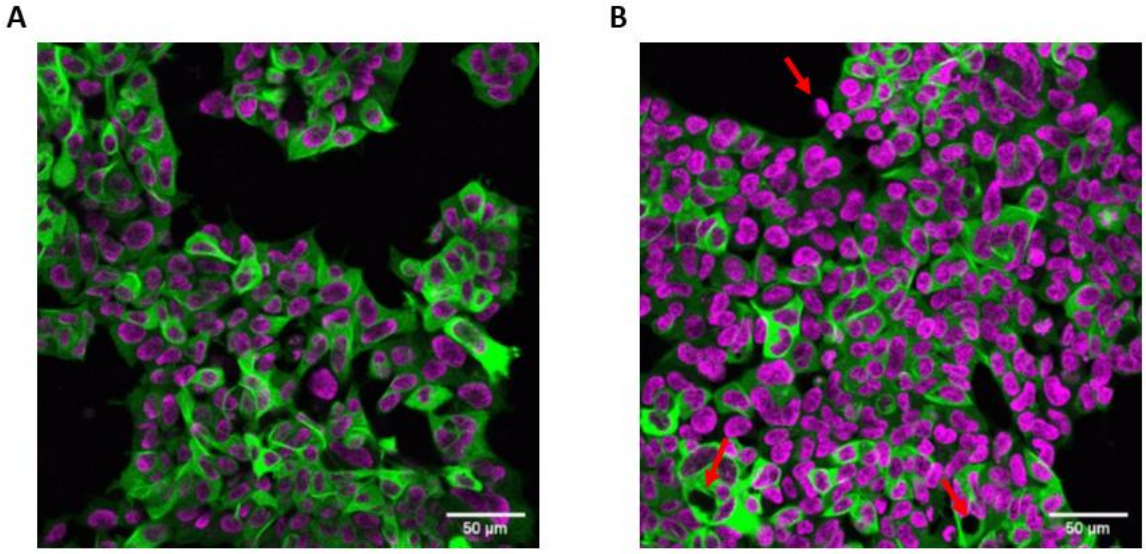

Figure 3.10 Tau Cells Stained with Hoechst 34580. A & B) Tau Cells stained with Hoechst 34580. Magenta represents the Hoechst dye fluorescing in the DAPI channel, and green is the EYFP signal imaged in the EYFP channel. Cells in A are of a higher quality with little variance in signal intensity. Cells in B are rounded, and their intensity varies. Cells indicated by the red arrows are cells with abnormal nuclei that suggest the cells are in poor health. These cells would be excluded from counting.

3.7 Biochemical Analysis of Protein Aggregates

To support the inhibitory findings produced by confocal microscopy, a biochemical assay of the tau aggregates was performed. Tau aggregates from cells are insoluble in mild detergents such as 1% Triton X-100 or 1% Sarkosyl solutions (47). This allows for the separation of tau aggregates from soluble monomer by sedimentation of cell lysates. Once sedimented, the pellets can be loaded on a 12% polyacrylamide gel, resolved by SDS-PAGE, and biochemically analyzed by Western Blot to quantify the amount of tau in pellets. In theory, one would expect to see a decrease in tau present in the pellets of cells that were given K18wt seeds preincubated with MAP2 vs cells that were given untreated

K18wt seeds. However, there have been complications with the pelleting procedure and only preliminary data using the supernatants has been produced (See Figure 3.11). This data confirms the antibodies function as desired and EYFP tagged tau can be detected. Further development of the triton insoluble pelleting procedure will be performed.

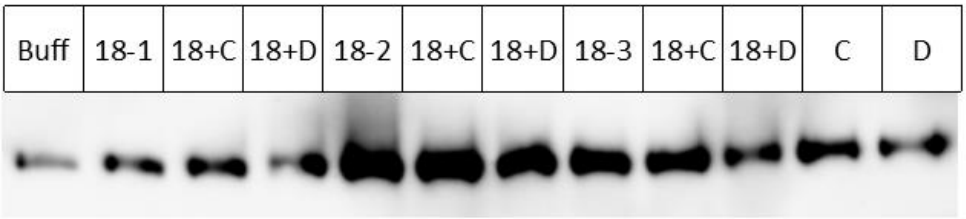

Figure 3.11 Western Blot of Supernatants of Tau Cells. Tau Cells were transfected with either a buffer control (Buff), K18wt seeds in triplicates, K18wt seeds preincubated with either MAP2Ctr or MAP2Dtr, MAP2Ctr alone, or MAP2Dtr alone. Cells were lysed in 1% Triton buffer and pelleted at 130,000 x g. Supernatants were resolved by SDS-PAGE, transferred onto blotting material, and blotted with rabbit anti-GFP Ab. A secondary goat anti-rabbit Ab conjugated to horse radish peroxidase was used for detection by chemiluminescence.

4. Chapter Four: Discussion

4.1 Established HEK293 Cell Lines Stably Expressing hT40P301S-EYFP and K18P301S-EYFP

The first goal of this project was to establish HEK293 cell lines that were stably transfected with and expressing hT40P301S-EYFP or K18P301S-EYFP. This was accomplished through lipofectamine transfection of pcDNA3.1 plasmid containing the genes of interest. After 1 week under selection media, the cells were imaged by confocal microscopy to confirm expression of the EYFP tagged K18P301S and hT40P301S. It was noted that K18P301S-EYFP cells had characteristics distinct from that of hT40P301S-EYFP. While K18P301S-EYFP was defuse within the cell, and even showed low fluorescence within the nucleus, it did not appear to localize to the microtubules. Interestingly, hT40P301S-EYFP appeared to interact strongly with microtubules allowing for the appearance of web-like structures within the cells. This suggest that the hT40P301S-EYFP could be performing its native function of stabilizing microtubules. This cannot be confirmed simply by this observation and further experiments, such as staining for microtubules and measuring colocalization, would further strengthen this hypothesis. The interaction of GFP tagged hT40wt with microtubules has been seen previously in PC12 cells (48). Although K18P301S-EYFP did not appear to

be interacting as strongly with microtubules as hT40P301S-EYFP, this does not mean it is not performing its native function. K18wt has a Kd of 25.5 μM for microtubule binding which is much higher than hT40wt's Kd of 1.1 μM (49). This means K18 has a much lower binding affinity for microtubules than hT40 does. It is possible that K18P301S-EYFP is in fact interacting with microtubules, but its on-off rate is too rapid for it to outline the microtubules as hT40P301S-EYFP does.

Although these cells are stably transfected and expressing the plasmid of interest, they were expressing the EYFP at varying levels. This difference is caused by various cells integrating a different number of plasmids into their genome, resulting in varying fluorescence intensity from cell to cell. Not only were the cells fluorescing at different intensities, but some were not fluorescing at all. It is possible that some cells have cleaved the plasmid within the gene of interest before integration. These cells can still express the resistance gene and thus survive the selection media, but do not express the gene of interest. Because of this, the cells were subjected to monoclonal selection to ensure the cells were fluorescing and that the intensity of fluorescence was consistent from cell to cell. Once the Tau Cells were selected, they were transfected with K18wt seeds to ensure that the hT40P301S-EYFP could be recruited onto the seeds and form intracellular puncta that could be viewed by confocal microscopy.

4.2 Stably Transfected Cells Produce Puncta when Transfected with K18wt Seeds

When hT40P301S-EYFP expressing cells were transfected with K18wt seeds, the web-like structures were often disrupted suggesting hT40P301S-EYFP was no longer interacting with the microtubule network. The EYFP fluorescence would cluster into distinct, bright, puncta of high intensity relative to the rest of the cell when seeds were present. These puncta were not observed in the absence of seeds when the cells were transfected with a buffer control, MAP2Ctr alone, or MAP2Dtr alone. The formation of puncta suggests that the hT40P301S-EYFP is no longer soluble but is instead being recruited onto the ends of the K18wt seeds and forming fibrils, resulting in a clustering of EYFP seen as bright puncta when viewed under confocal microscopy. It has previously been observed that hT40P301S is capable of being recruited by K18wt seeds in culture, and this holds true for our EYFP tagged construct (50). K18P301S-EYFP cells were both capable of forming puncta when transfected with K18wt seeds (See Appendix C). K18P301S-EYFP cells showed unique puncta morphology when the cells were transfected with K18wt seeds from those formed by hT40P301S-EYFP. While K18P301S-EYFP formed relatively large and often singular puncta within cells, hT40P301S-EYFP was observed to form many more, smaller, diffuse puncta within cells as well as larger puncta. When viewed under confocal microscopy, these smaller puncta formed by hT40P301S-EYFP could be seen being shuttled around the cell whereas the larger hT40P301S-

EYFP were stationary. This shuttling of small aggregates was not observed for K18P301S-EYFP. Similar diversity in puncta morphology has been observed previously in other tau models (51). The difference in puncta morphology could be due to the presence of the N- and C-termini in the hT40P301S-EYFP construct. It would be interesting to see how the morphology of puncta may differ for other seed types that have been shown to have different conformations than K18wt. For example, how do these puncta look and behave for seeds composed of hT40wt monomer? hT40wt fibrils show more order in the 4R than K18wt fibrils do and this change in conformation could result in unique puncta morphology (52). Now that it has been shown that K18wt seeds can recruit hT40P301S-YFP to form intracellular puncta in HEK293 cells, we wanted to see if puncta formation could be inhibited by MAP2Ctr and MAP2Dtr.

4.3 Inhibition of Intracellular Puncta Formation by MAP2Ctr and MAP2Dtr

Tau Cells were transfected with seeds that were either preincubated with MAP2Ctr, MAP2Dtr, or just buffer. The cells that received seeds that had been preincubated with MAP2 showed a significant reduction in cells containing puncta with MAP2Dtr being able to decrease cells containing puncta by 54.3%. This suggest a potential mechanism of inhibiting tau fibril elongation by out-competing hT40P301S-EYFP recruitment. Further investigation into the precise sequence of

MAP2 responsible for this inhibitory mechanism is needed as it could produce a smaller peptide that would inhibit tau fibril elongation.

Cells that were treated with K18wt seeds, either treated or not, had an overall higher fluorescent intensity than the control cells. This could be due to the pcDNA3.1 plasmid used for transfection of the hT40P301S-EYFP construct. The pcDNA3.1 plasmid contains a cytomegalovirus (CMV) enhance-promoter for high expression levels of the gene of interest. This promoter is enhanced by transcription factors such as cAMP response element-binding protein, activator protein 1, and specific protein 1, all of which are involved in stress response within the cell (53). This could lead to increased expression levels of hT40P301S-YFP as a response to the toxic aggregates (54).

It was also noted that the ability for MAP2 to inhibit puncta formation in culture was lost over time (data not shown). The K18wt seeds were preincubated with MAP2Ctr and MAP2Dtr before being transfected into the cells. Due to this method of treating the seeds, the supply of MAP2Ctr and MAP2Dtr is cut off post-transfection. To the contrary there is a constant supply of hT40P301S-EYFP within the cells. The resulting effect is that any K18wt seed that was not capped, or the MAP2 dissociated from its end, has the propensity to elongate, fracture, and spread, not only intracellularly but potentially intercellularly as well (34). MAP2 could be removed from the fibrils by proteolytic means, or fibrils could be fractured potentially by chaperones, exposing new ends that could recruit tau (55, 56).

4.4 Further Investigation into in-culture Inhibition Effects of MAP2Ctr and MAP2Dtr

To improve upon the confocal findings, Hoechst 34580 dye was used to stain the nuclei of cells and assist in more consistent and accurate cell counting. Currently, the dye is added directly to the media after the full 12h incubation. The dye is incubated cells for 10 min at 37 ºC so the dye can permeate the cells. The media is changed following the 10 min incubation to remove any excess dye. This protocol has greatly improved the quality of images and the over health of the cells. Previous methods had led to the cells being washed away or damaged in the process. However, even with the improvements made to the protocol, the images are still not of a quality comparable to those that had not been dyed. One way to improve upon this problem could be to coat the plate with poly-D-lysine. This could adhere the cells more strongly to the plate and prevent them from being washed away (54). Another possible solution could be to lower the dye concentration and allow for a longer recovery period after staining.

We also sought to show the reduction of tau aggregation in culture through a biochemical assay. Tau aggregates are insoluble in 1% Triton X-100 or sarkosyl solutions and several labs have exploited this to separate aggregates from monomeric tau in culture (47, 57–59). I sought to use this method to isolate aggregates from cells to show a reduction in EYFP labeled tau in the pellets when the cells were transfected with treated seeds. However, the protocol needs further improvements. Currently, a 1% Triton X-100 solution is being used, but a

1% sarkosyl solution could be used instead if the triton solution continues to be unsuccessful.

4.5 Summary

The goal of this project was to establish a human cell line that could test in culture inhibition of tau aggregation by MAP2Ctr and MAP2Dtr. HEK293 cell lines stably expressing K18P301S-EYFP or hT40P301S-EYFP were successfully established and a monoclonal cell line expressing hT40P301S-EYFP was selected. The hT40P301S-EYFP cell line was used to show that when transfected with K18wt seeds, the seeds could successfully recruit hT40P301S-EYFP to form intracellular puncta. The hT40P301S-EYFP cell line was then used to show in culture inhibition of tau aggregation by MAP2Ctr and MAP2Dtr. This cell line is a powerful model that can be used for future research within the lab.

5. References

1. C.F., P., Yen Ng, K., Yian Koh, R., and Moi Chye, S. (2018) Tau Proteins and Tauopathies in Alzheimer's Disease. *Cell. Mol. Neurobiol.* **38**, 965–980
2. Bloom, G. S. (2014) Amyloid-β and Tau. *JAMA Neurol.* **71**, 505–508
3. Martin Prince, A., Wimo, A., Guerchet, M., Gemma-Claire Ali, M., Wu, Y.-T., Prina, M., Yee Chan, K., and Xia, Z. (2015) *World Alzheimer Report 2015 The Global Impact of Dementia An An Analysis of Prevalence, Incidence, Cost and Trends*
4. Matthews, K. A., Xu, W., Gaglioti, A. H., Holt, J. B., Croft, J. B., Mack, D., and McGuire, L. C. (2019) Racial and Ethnic Estimates of Alzheimer's Disease and Related Dementias in The United States (2015–2060) in Adults Aged ≥65 Years. *Alzheimer's Dement.* **15**, 17–24
5. Alzheimer's Facts and Figures Report | Alzheimer's Association
6. Duan, A. R., Jonasson, E. M., Alberico, E. O., Li, C., Scripture, J. P., Miller, R. A., Alber, M. S., and Goodson, H. V. (2017) Interactions between Tau and Different Conformations of Tubulin: Implications for Tau Function and Mechanism. *J. Mol. Biol.* **429**, 1424–1438
7. Callahan, L. M., Vaules, W. A., and Coleman, P. D. (2002) Progressive Reduction of Synaptophysin Message in Single Meurons in Alzheimer Disease. *J. Neuropathol. Exp. Neurol.* **61**, 384–95
8. Wright, P. E., and Jane Dyson, H. (2015) Intrinsically Disordered Proteins in Cellular Signalling and Regulation. *Nat. Publ. Gr.* **16**, 18–29
9. Dunker, A. K., Lawson, J. D., Brown, C. J., Williams, R. M., Romero, P., Oh, J. S., Oldfield, C. J., Campen, A. M., Ratliff, C. M., Hipps, K. W., Ausio, J., Nissen, M. S., Reeves, R., Kang, C., Kissinger, C. R., Bailey, R. W., Griswold, M. D., Chiu, W., Garner, E. C., and Obradovic, Z. (2001) Intrinsically Disordered Protein. *J. Mol. Graph. Model.* **19**, 26–59
10. Uversky, V. N., Oldfield, C. J., and Dunker, A. K. (2008) Intrinsically Disordered Proteins in Human Diseases: Introducing the D2 Concept. *Annu. Rev. Biophys.* **37**, 215–246
11. Jeganathan, S., Bergen, M. von, Brutlach, H., Heinz-Jürgen Steinhoff, A., and Mandelkow, E. (2006) Global Hairpin Folding of Tau in Solution. *Biochemistry*. **45**, 2283–2293
12. Jeganathan, S., Hascher, A., Chinnathambi, S., Biernat, J., Mandelkow, E.-M., and Mandelkow, E. (2008) Proline-directed Pseudo-phosphorylation at AT8 and PHF1 Epitopes Induces a Compaction of the Paperclip Folding of Tau and Generates a Pathological (MC-1) Conformation. *J. Biol. Chem.* **283**, 32066–32076
13. Goedert, M., Spillantini, M. G., Jakes, R., Rutherford, D., and Crowther, R. A. (1989) Multiple Isoforms of Human Microtubule-Associated Protein Tau: Sequences and Localization in Neurofibrillary Tangles of Alzheimer's Disease. *Neuron*. **3**, 519–526

14. Goedert, M., and Jakes, R. (1990) Expression of Separate Isoforms of Human Tau Protein: Correlation With the Tau Pattern in Brain and Effects on Tubulin Polymerization. *EMBO J.* **9**, 4225–4230
15. Buée, L., Bussière, T., Buée-Scherrer, V., Delacourte, A., and Hof, P. R. (2000) Tau Protein Isoforms, Phosphorylation and Role in Neurodegenerative Disorders. *Brain Res. Rev.* **33**, 95–130
16. Janke, C., Beck, M., Stahl, T., Holzer, M., Brauer, K., Bigl, V., and Arendt, T. (1999) Phylogenetic Diversity of The Expression of The Microtubule-Associated Protein Tau: Implications for Neurodegenerative Disorders. *Mol. Brain Res.* **68**, 119–128
17. Mondragón-Rodríguez, S., Basurto-Islas, G., Santa-Maria, I., Mena, R., Binder, L. I., Avila, J., Smith, M. A., Perry, G., and García-Sierra, F. (2008) Cleavage and Conformational Changes of Tau Protein Follow Phosphorylation During Alzheimer's Disease. *Int. J. Exp. Pathol.* **89**, 81–90
18. Kanaan, N. M., Morfini, G. A., LaPointe, N. E., Pigino, G. F., Patterson, K. R., Song, Y., Andreadis, A., Fu, Y., Brady, S. T., and Binder, L. I. (2011) Pathogenic Forms of Tau Inhibit Kinesin-Dependent Axonal Transport through a Mechanism Involving Activation of Axonal Phosphotransferases. *J. Neurosci.* **31**, 9858–9868
19. Carmen N. Chirita, Congdon, E. E., Haishan Yin, A., and Kuret, J. (2005) Triggers of Full-Length Tau Aggregation: A Role for Partially Folded Intermediates. *Biochemistry*. **44**, 5862–5872
20. Maeda, S., Sahara, N., Saito, Y., Murayama, M., Yoshiike, Y., Kim, H., Miyasaka, T., Murayama, S., Atsushi Ikai, A., and Takashima, A. (2007) Granular Tau Oligomers as Intermediates of Tau Filaments. *Biochemistry*. **46**, 3856–3861
21. Congdon, E. E., Kim, S., Bonchak, J., Songrug, T., Matzavinos, A., and Kuret, J. (2008) Nucleation-Dependent Tau Filament Formation: The Importance of Dimerization and an Estimation of Elementary Rate Constants. *J. Biol. Chem.* **283**, 13806–16
22. Mirbaha, H., Chen, D., Morazova, O. A., Ruff, K. M., Sharma, A. M., Liu, X., Goodarzi, M., Pappu, R. V., Colby, D. W., Mirzaei, H., Joachimiak, L. A., and Diamond, M. I. (2018) Inert and Seed-Competent Tau Monomers Suggest Structural Origins of Aggregation. *Elife*. **7**, 1–29
23. Meyer, V., Holden, M. R., Weismiller, H. A., Eaton, G. R., Eaton, S. S., and Margittai, M. (2016) Fracture and Growth Are Competing Forces Determining the Fate of Conformers in Tau Fibril Populations. *J. Biol. Chem.* **291**, 122271–12281
24. Kidd, M. (1963) Paired Helical Filaments in Electron Microscopy of Alzheimer's Disease. *Nature*. **197**, 192–193
25. Yagishita, S., Itoh, Y., Nan, W., and Amano, N. (1981) Reappraisal of the fine structure of Alzheimer's neurofibrillary tangles. *Acta Neuropathol.* **54**, 239–246

26. Novak, M., Kabat, J., and Wischik, C. M. (1993) Molecular Characterization of The Minimal Protease Resistant Tau Unit of The Alzheimer's Disease Paired Helical Filament. *EMBO J.* **12**, 365–370
27. Margittai, M., and Langen, R. (2008) Fibrils with Parallel In-Register Structure Constitute a Major Class of Amyloid Fibrils: Molecular Insights from Electron Paramagnetic Resonance Spectroscopy. *Q. Rev. Biophys.* **41**, 265–297
28. Margittai, M., and Langen, R. (2004) Template-Assisted Filament Growth by Parallel Stacking of Tau. *Proc. Natl. Acad. Sci.* **101**, 10278–10283
29. Friedhoff, P., Schneider, A., Mandelkow, E. M., and Mandelkow, E. (1998) Rapid Assembly of Alzheimer-like Paired Helical Filaments from Microtubule-Associated Protein Tau Monitored by Fluorescence in Solution. *Biochemistry*. **37**, 10223–10230
30. Kampers, T., Friedhoff, P., Biernat, J., Mandelkow, E.-M., and Mandelkow, E. (1996) RNA Stimulates Aggregation of Microtubule-Associated Protein Tau into Alzheimer-Like Paired Helical Filaments. *FEBS Lett.* **399**, 344–349
31. King, M. E., Gamblin, T. C., Kuret, J., and Binder, L. I. (2002) Differential Assembly of Human Tau Isoforms in the Presence of Arachidonic Acid. *J. Neurochem.* **74**, 1749–1757
32. Gerson, J. E., and Kayed, R. (2013) Formation and Propagation of Tau Oligomeric Seeds. *Front. Neurol.* **4**, 93
33. Sanders, D. W., Kaufman, S. K., DeVos, S. L., Sharma, A. M., Mirbaha, H., Li, A., Barker, S. J., Foley, A. C., Thorpe, J. R., Serpell, L. C., Miller, T. M., Grinberg, L. T., Seeley, W. W., and Diamond, M. I. (2014) Distinct Tau Prion Strains Propagate in Cells and Mice and Define Different Tauopathies. *Neuron*. **82**, 1271–1288
34. Mirbaha, H., Holmes, B. B., Sanders, D. W., Bieschke, J., and Diamond, M. I. (2015) Tau Trimers Are the Minimal Propagation Unit Spontaneously Internalized to Seed Intracellular Aggregation. *J. Biol. Chem.* **290**, 14893–903
35. Sievers, S. A., Karanicolas, J., Chang, H. W., Zhao, A., Jiang, L., Zirafi, O., Stevens, J. T., Münch, J., Baker, D., and Eisenberg, D. (2011) Structure-Based Design of Non-Natural Amino-Acid Inhibitors of Amyloid Fibril Formation. *Nature*. **475**, 96–103
36. Seidler, P. M., Boyer, D. R., Rodriguez, J. A., Sawaya, M. R., Cascio, D., Murray, K., Gonen, T., Eisenberg, D. S., and Author, N. C. (2018) Structure-Based Inhibitors of Tau Aggregation. *Nat Chem*. **10**, 170–176
37. Tucker, R. P. (1990) The Roles of Microtubule-Associated Proteins in Brain Morphogenesis: A Review. *Brain Res. Rev.* **15**, 101–120
38. Dehmelt, L., and Halpain, S. (2005) The MAP2/Tau Family of Microtubule-Associated Proteins. *Genome Biol.* **6**, 204–214
39. Uchida, Y., Ihara, Y., and Tomonaga, M. (1988) Alzheimer's Disease Brain

Extract Stimulates the Survival of Cerebral Cortical Neurons from Neonatal Rats. *Biochem. Biophys. Res. Commun.* **150**, 1263–1267
40. Mailliot, C., Bussière, T., Caillet-Boudin, M.-L., Delacourte, A., and Buée, L. (1998) Alzheimer-Specific Epitope of AT100 in Transfected Cell Lines With Tau: Toward an Efficient Cell Model of Tau Abnormal Phosphorylation. *Neurosci. Lett.* **255**, 13–16
41. Pickhardt, M., Gazova, Z., Von Bergen, M., Khlistunova, I., Wang, Y., Hascher, A., Mandelkow, E.-M., Biernat, J., and Mandelkow, E. (2005) Anthraquinones Inhibit Tau Aggregation and Dissolve Alzheimer's Paired Helical Filaments in Vitro and in Cells. *J. Biol. Chem.* **280**, 3628–3635
42. Liu, R., Yu, G., Li, Y., Tian, Q., Wang, Q., Wang, J.-Z., and Wang, X. (2011) Brberine Attenuates Calyculin A-Induced Cytotoxicity and Tau Hyperphosphorylation in HEK293 Cells. *J. Alzheimer's Dis.* **24**, 525–535
43. Yanamandra, K., Kfoury, N., Jiang, H., Mahan, T. E., Ma, S., Maloney, S. E., Wozniak, D. F., Diamond, M. I., and Holtzman, D. M. (2013) Anti-Tau Antibodies that Block Tau Aggregate Seeding In Vitro Markedly Decrease Pathology and Improve Cognition In Vivo. *Neuron*. **80**, 402–414
44. Goedert, M., and Spillantini, M. G. (2017) Propagation of Tau aggregates. *Mol. Brain*. **10**, 1–9
45. Schneider, C. A., Rasband, W. S., and Eliceiri, K. W. (2012) NIH Image to ImageJ: 25 years of image analysis. *Nat. Methods*. **9**, 671–675
46. Southern, P. J., and Berg, P. (1982) Transformation of mammalian cells to antibiotic resistance with a bacterial gene under control of the SV40 early region promoter. *J. Mol. Appl. Genet.* **1**, 327–41
47. Strang, K. H., Croft, C. L., Sorrentino, Z. A., Chakrabarty, P., Golde, T. E., Giasson, B. I., and Fraser, P. E. (2018) Distinct Differences in Prion-Like Seeding and Aggregation Between Tau Protein Variants Provide Mechanistic Insights into Tauopathies. *J. Biol. Chem.* **293**, 2408–2421
48. Weissmann, C., Reyher, H. J., Gauthier, A., Steinhoff, H. J., Junge, W., and Brandt, R. (2009) Microtubule binding and trapping at the tip of neurites regulate tau motion in living neurons. *Traffic*. **10**, 1655–1668
49. Gustke, N., Trinczek, B., Biernat, J., Mandelkow, E.-M., and Mandelkow, E. (1994) Domains of tau Protein and Interactions with Microtubules. *Biochemistry*. **33**, 9511–9522
50. Strang, K. H., Croft, C. L., Sorrentino, Z. A., Chakrabarty, P., Golde, T. E., and Giasson, B. I. (2018) Distinct differences in prion-like seeding and aggregation between Tau protein variants provide mechanistic insights into tauopathies. *J. Biol. Chem.* **293**, 2408–2421
51. Kaufman, S. K., Sanders, D. W., Thomas, T. L., Ruchinskas, A. J., Vaquer-Alicea, J., Sharma, A. M., Miller, T. M., and Diamond, M. I. (2016) Tau Prion Strains Dictate Patterns of Cell Pathology, Progression Rate, and Regional Vulnerability In Vivo. *Neuron*. **92**, 796–812
52. Weismiller, H. A., Murphy, R., Wei, G., Ma, B., Nussinov, R., and Margittai,

M. (2018) Structural Disorder in Four-Repeat Tau Fibrils Reveals a New Mechanism for Barriers to Cross-Seeding of Tau Isoforms. *J. Biol. Chem.* **293**, 17336–17348

53. Isomura, H., and Stinski, M. F. (2003) The Human Cytomegalovirus Major Immediate-Early Enhancer Determines The Efficiency of Immediate-Early Gene Transcription and Viral Replication in Permissive Cells at Low Multiplicity of Infection. *J. Virol.* **77**, 3602–14
54. Bruening, W., Giasson, B., Mushynski, W., and Durham, H. D. (1998) Activation of Stress-Activated MAP Protein Kinases Up-Regulates Expression of Transgenes Driven by The Cytomegalovirus Immediate/Early Promoter. *Nucleic Acids Res.* **26**, 486–489
55. Celli, V., Eichenauer, D., Kaufhold, A., Toennies, J. P., Shorter, J., and Lindquist, S. (2004) Hsp104 Catalyzes Formation and Elimination of Self-Replicating Sup35 Prion Conformers. *J. Phys. Condens. Matter*. **304**, 1793–1797
56. Shorter, J., and Lindquist, S. Destruction or Potentiation of Different Prions Catalyzed by Similar Hsp104 Remodeling Activities. *Mol. Cell*. **23**, 425–438
57. Frost, B., Jacks, R. L., and Diamond, M. I. (2009) Propagation of Tau Misfolding from the Outside to the Inside of a Cell. *J. Biol. Chem.* **284**, 12845–12852
58. Nonaka, T., Watanabe, S. T., Iwatsubo, T., and Hasegawa, M. (2010) Seeded Aggregation and Toxicity of-Synuclein and Tau. *J. Biol. Chem.* **285**, 34885–34898
59. Guo, J. L., and M-Y Lee, V. (2011) Seeding of Normal Tau by Pathological Tau Conformers Drives Pathogenesis of Alzheimer-like Tangles. *J. Biol. Chem.* **286**, 15317–15331

6. Appendix A: Construct Sequences

MAP2Ctr DNA Sequence:

CGCCTGATTAATCAGCCTTTACCGGATCTGAAAAATGTTAAATCTAAAATCG
GCTCTACGGATAATATCAAATATCAGCCTAAAGGTGGTCAGGTTCAGATTGT
GACCAAAAAGATCGATCTGTCACATGTGACGAGTAAATGCGGTTCACTGAAA
AATATCCGTCATAGGCCAGGTGGCGGTCGTGTTAAAATCGAATCTGTTAAAC
TGGATTTTAAAGAAAAAGCGCAGGCCAAAGTGGGTTCTTTAGATAATGCCCA
TCATGTTCCGGGTGGCGGTAATGTTAAA

MAP2Dtr DNA Sequence:

CGTCTGATTAATCAGCCTCTGCCGGATCTGAAAAATGTTAAATCTAAAATTG
GCTCAACCGATAATATCAAATATCAGCCTAAAGGCGGTCAGGTTCGCATCCT
GAACAAGAAGATCGATTTTAGCAAAGTGCAGTCACGTTGCGGCAGTAAAGA
TAATATCAAACATAGCGCCGGCGGAGGTAATGTGCAGATTGTGACCAAGAA
GATCGATCTGTCACATGTGACAAGTAAATGCGGTTCACTGAAAAATATTCGT
CATCGTCCGGGTGGCGGTCGTGTTAAAATCGAATCAGTTAAACTGGATTTTA
AAGAAAAAGCCCAGGCCAAAGTGGGCTCACTGGATAATGCACATCATGTTC
CAGGTGGTGGCAATGTTAAAATTGAT

hT40P301S-EYFP DNA Sequence:
AAGCTTACCATGGCTGAGCCCCGCCAGGAGTTCGAAGTGATGGAAGATCAC
GCTGGGACGTACGGGTTGGGGGACAGGAAAGATCAGGGGGGCTACACCAT
GCACCAAGACCAAGAGGGTGACACGGACGCTGGCCTGAAAGAATCTCCCC
TGCAGACCCCCACTGAGGACGGATCTGAGGAACCGGGCTCTGAAACCTCT
GATGCTAAGAGCACTCCAACAGCGGAAGATGTGACAGCACCCTTAGTGGAT
GAGGGAGCTCCCGGCAAGCAGGCTGCCGCGCAGCCCCACACGGAGATCC
CAGAAGGAACCACAGCTGAAGAAGCAGGCATTGGAGACACCCCCAGCCTG
GAAGACGAAGCTGCTGGTCACGTGACCCAAGCTCGCATGGTCAGTAAAAGC
AAAGACGGGACTGGAAGCGATGACAAAAAAGCCAAGGGGGCTGATGGTAA
AACGAAGATCGCCACACCGCGGGGAGCAGCCCCTCCAGGCCAGAAGGGC
CAGGCCAACGCCACCAGGATTCCAGCAAAAACCCCGCCCGCTCCAAAGAC
ACCACCCAGCTCTGGTGAACCTCCAAAATCAGGGGATCGCAGCGGCTACA
GCAGCCCCGGCTCCCCAGGCACTCCCGGCAGCCGCTCCCGCACCCCGTC
CCTTCCAACCCCACCCACCCGGGAGCCCAAGAAGGTGGCAGTGGTCCGTA
CTCCACCCAAGTCGCCGTCTTCCGCCAAGAGCCGCCTGCAGACAGCCCCC
GTGCCCATGCCAGACCTGAAGAATGTCAAGTCCAAGATCGGCTCCACTGAG
AACCTGAAGCACCAGCCGGGAGGCGGGAAGGTGCAGATAATTAATAAGAA
GCTGGATCTTAGCAACGTCCAGTCCAAGTGTGGCTCAAAGGATAATATCAAA
CACGTCAGCGGAGGCGGCAGTGTGCAAATAGTCTACAAACCAGTTGACCTG
AGCAAGGTGACCTCCAAGTGTGGCTCATTAGGCAACATCCATCATAAACCA

GGAGGTGGCCAGGTGGAAGTAAAATCTGAGAAGCTGGACTTCAAGGACAG
AGTCCAGTCGAAGATTGGGTCCCTGGACAATATCACCCACGTCCCTGGCGG
AGGAAATAAAAAGATTGAAACCCACAAGCTGACCTTCCGCGAGAACGCCAA
AGCCAAGACAGACCACGGGGCGGAGATCGTGTACAAGTCGCCAGTGGTGT
CTGGGGACACGTCTCCACGGCATCTCAGCAATGTCTCCTCCACCGGCAGCA
TCGACATGGTAGACTCGCCCCAGCTCGCCACGCTAGCTGACGAGGTGTCT
GCCTCCCTGGCCAAGCAGGGTTTGGGCGGAGGCGGGAGCGGCGGAGGCG
GAAGCGGCGGCGGAGGCAGCGGCGGCGGAGGATCCATGGTGAGCAAGGG
CGAGGAGCTGTTCACCGGGGTGGTGCCCATCCTGGTCGAGCTGGACGGCG
ACGTAAACGGCCACAAGTTCAGCGTGTCCGGCGAGGGCGAGGGCGATGCC
ACCTACGGCAAGCTGACCCTGAAGTTCATCTGCACCACCGGCAAGCTGCCC
GTGCCCTGGCCCACCCTCGTGACCACCTTCGGCTACGGCCTGCAGTGCTT
CGCCCGCTACCCCGACCACATGAAGCAGCACGACTTCTTCAAGTCCGCCAT
GCCCGAAGGCTACGTCCAGGAGCGCACCATCTTCTTCAAGGACGACGGCA
ACTACAAGACCCGCGCCGAGGTGAAGTTCGAGGGCGACACCCTGGTGAAC
CGCATCGAGCTGAAGGGCATCGACTTCAAGGAGGACGGCAACATCCTGGG
GCACAAGCTGGAGTACAACTACAACAGCCACAACGTCTATATCATGGCCGA
CAAGCAGAAGAACGGCATCAAGGTGAACTTCAAGATCCGCCACAACATCGA
GGACGGCAGCGTGCAGCTCGCCGACCACTACCAGCAGAACACCCCCATCG
GCGACGGCCCCGTGCTGCTGCCCGACAACCACTACCTGAGCTACCAGTCC
GCCCTGAGCAAAGACCCCAACGAGAAGCGCGATCACATGGTCCTGCTGGA
GTTCGTGACCGCCGCCGGGATCACTCTCGGCATGGACGAGCTGTACAAGT
AATGATAACTCGAG

hT40P301S-EYFP Amino Acid Sequence:

MAEPRQEFEVMEDHAGTYGLGDRKDQGGYTMHQDQEGDTDAGLKESPLQTP
TEDGSEEPGSETSDAKSTPTAEDVTAPLVDEGAPGKQAAAQPHTEIPEGTTAE
EAGIGDTPSLEDEAAGHVTQARMVSKSKDGTGSDDKKAKGADGKTKIATPRGA
APPGQKGQANATRIPAKTPPAPKTPPSSGEPPKSGDRSGYSSPGSPGTPGSR
SRTPSLPTPPTREPKKVAVVRTPPKSPSSAKSRLQTAPVPMPDLKNVKSKIGST
ENLKHQPGGGKVQIINKKLDLSNVQSKCGSKDNIKHVSGGGSVQIVYKPVDLSK
VTSKCGSLGNIHHKPGGGQVEVKSEKLDFKDRVQSKIGSLDNITHVPGGGNKKI
ETHKLTFRENAKAKTDHGAEIVYKSPVVSGDTSPRHLSNVSSTGSIDMVDSPQL
ATLADEVSASLAKQGLGGGGSGGGGSGGGGSGGGGSMVSKGEELFTGVVPI
LVELDGDVNGHKFSVSGEGEGDATYGKLTLKFICTTGKLPVPWPTLVTTFGYGL
QCFARYPDHMKQHDFFKSAMPEGYVQERTIFFKDDGNYKTRAEVKFEGDTLV
NRIELKGIDFKEDGNILGHKLEYNYNSHNVYIMADKQKNGIKVNFKIRHNIEDGSV
QLADHYQQNTPIGDGPVLLPDNHYLSYQSALSKDPNEKRDHMVLLEFVTAAGIT
LGMDELYK

Red denotes the amino acid sequence of K18P301S, the blue denotes the linker sequences used to link K18P301S to YFP, and the yellow is the amino acid sequence for YFP.

K18P301S-EYFP DNA Sequnce:

AAGCTTACCATGGGCCAGACAGCCCCCGTGCCCATGCCAGACCTGAAGAAT
GTCAAGTCCAAGATCGGCTCCACTGAGAACCTGAAGCACCAGCCGGGAGG
CGGGAAGGTGCAGATAATTAATAAGAAGCTGGATCTTAGCAACGTCCAGTC
CAAGTGTGGCTCAAAGGATAATATCAAACACGTCAGCGGAGGCGGCAGTGT
GCAAATAGTCTACAAACCAGTTGACCTGAGCAAGGTGACCTCCAAGTGTGG
CTCATTAGGCAACATCCATCATAAACCAGGAGGTGGCCAGGTGGAAGTAAA
ATCTGAGAAGCTGGACTTCAAGGACAGAGTCCAGTCGAAGATTGGGTCCCT
GGACAATATCACCCACGTCCCTGGCGGAGGAAATAAAAAGATTGAAGGCGG
AGGCGGGAGCGGCGGAGGCGGAAGCGGCGGCGGAGGCAGCGGCGGCGG
AGGATCCATGGTGAGCAAGGGCGAGGAGCTGTTCACCGGGGTGGTGCCCA
TCCTGGTCGAGCTGGACGGCGACGTAAACGGCCACAAGTTCAGCGTGTCC
GGCGAGGGCGAGGGCGATGCCACCTACGGCAAGCTGACCCTGAAGTTCAT
CTGCACCACCGGCAAGCTGCCCGTGCCCTGGCCCACCCTCGTGACCACCT
TCGGCTACGGCCTGCAGTGCTTCGCCCGCTACCCCGACCACATGAAGCAG
CACGACTTCTTCAAGTCCGCCATGCCCGAAGGCTACGTCCAGGAGCGCAC
CATCTTCTTCAAGGACGACGGCAACTACAAGACCCGCGCCGAGGTGAAGTT
CGAGGGCGACACCCTGGTGAACCGCATCGAGCTGAAGGGCATCGACTTCA
AGGAGGACGGCAACATCCTGGGGCACAAGCTGGAGTACAACTACAACAGC
CACAACGTCTATATCATGGCCGACAAGCAGAAGAACGGCATCAAGGTGAAC
TTCAAGATCCGCCACAACATCGAGGACGGCAGCGTGCAGCTCGCCGACCA
CTACCAGCAGAACACCCCCATCGGCGACGGCCCCGTGCTGCTGCCCGACA
ACCACTACCTGAGCTACCAGTCCGCCCTGAGCAAAGACCCCAACGAGAAGC
GCGATCACATGGTCCTGCTGGAGTTCGTGACCGCCGCCGGGATCACTCTC
GGCATGGACGAGCTGTACAAGTAATGATAACTCGAG

K18P301S-EYFP Amino Acid Sequence:

MGQTAPVPMPDLKNVKSKIGSTENLKHQPGGGKVQIINKKLDLSNVQSKCGSK
DNIKHVSGGGSVQIVYKPVDLSKVTSKCGSLGNIHHKPGGGQVEVKSEKLDFK
DRVQSKIGSLDNITHVPGGGNKKIEGGGGSGGGGSGGGGSGGGGSMVSKGE
ELFTGVVPILVELDGDVNGHKFSVSGEGEGDATYGKLTLKFICTTGKLPVPWPT
LVTTFGYGLQCFARYPDHMKQHDFFKSAMPEGYVQERTIFFKDDGNYKTRAEV
KFEGDTLVNRIELKGIDFKEDGNILGHKLEYNYNSHNVYIMADKQKNGIKVNFKI
RHNIEDGSVQLADHYQQNTPIGDGPVLLPDNHYLSYQSALSKDPNEKRDHMVL
LEFVTAAGITLGMDELYK

Red denotes the amino acid sequence of K18P301S, the blue denotes the linker sequences used to link K18P301S to YFP, and the yellow is the amino acid sequence for YFP.

hT40wt DNA Sequence:

ATGGCTGAGCCCCGCCAGGAGTTCGAAGTGATGGAAGATCACGCTGGGAC
GTACGGGTTGGGGGACAGGAAAGATCAGGGGGGCTACACCATGCACCAAG
ACCAAGAGGGTGACACGGACGCTGGCCTGAAAGAATCTCCCCTGCAGACC
CCCACTGAGGACGGATCTGAGGAACCGGGCTCTGAAACCTCTGATGCTAAG
AGCACTCCAACAGCGGAAGATGTGACAGCACCCTTAGTGGATGAGGGAGC
TCCCGGCAAGCAGGCTGCCGCGCAGCCCCACACGGAGATCCCAGAAGGAA
CCACAGCTGAAGAAGCAGGCATTGGAGACACCCCCAGCCTGGAAGACGAA
GCTGCTGGTCACGTGACCCAAGCTCGCATGGTCAGTAAAAGCAAAGACGG
GACTGGAAGCGATGACAAAAAAGCCAAGGGGGCTGATGGTAAAACGAAGAT
CGCCACACCGCGGGGAGCAGCCCCTCCAGGCCAGAAGGGCCAGGCCAAC
GCCACCAGGATTCCAGCAAAAACCCCGCCCGCTCCAAAGACACCACCCAG
CTCTGGTGAACCTCCAAAATCAGGGGATCGCAGCGGCTACAGCAGCCCCG
GCTCCCCAGGCACTCCCGGCAGCCGCTCCCGCACCCCGTCCCTTCCAACC
CCACCCACCCGGGAGCCCAAGAAGGTGGCAGTGGTCCGTACTCCACCCAA
GTCGCCGTCTTCCGCCAAGAGCCGCCTGCAGACAGCCCCCGTGCCCATGC
CAGACCTGAAGAATGTCAAGTCCAAGATCGGCTCCACTGAGAACCTGAAGC
ACCAGCCGGGAGGCGGGAAGGTGCAGATAATTAATAAGAAGCTGGATCTTA
GCAACGTCCAGTCCAAGAGCGGCTCAAAGGATAATATCAAACACGTCCCGG
GAGGCGGCAGTGTGCAAATAGTCTACAAACCAGTTGACCTGAGCAAGGTGA
CCTCCAAGAGCGGCTCATTAGGCAACATCCATCATAAACCAGGAGGTGGCC
AGGTGGAAGTAAAATCTGAGAAGCTTGACTTCAAGGACAGAGTCCAGTCGA
AGATTGGGTCCCTGGACAATATCACCCACGTCCCTGGCGGAGGAAATAAAA
AGATTGAAACCCACAAGCTGACCTTCCGCGAGAACGCCAAAGCCAAGACAG
ACCACGGGGCGGAGATCGTGTACAAGTCGCCAGTGGTGTCTGGGGACACG
TCTCCACGGCATCTCAGCAATGTCTCCTCCACCGGCAGCATCGACATGGTA
GACTCGCCCCAGCTCGCCACGCTAGCTGACGAGGTGTCTGCCTCCCTGGC
CAAGCAGGGTTTG

K18wt DNA Sequence:

ATGGGCCAGACAGCCCCCGTGCCCATGCCAGACCTGAAGAATGTCAAGTC
CAAGATCGGCTCCACTGAGAACCTGAAGCACCAGCCGGGAGGCGGGAAGG
TGCAGATAATTAATAAGAAGCTGGATCTTAGCAACGTCCAGTCCAAGTGTGG
CTCAAAGGATAATATCAAACACGTCAGCGGAGGCGGCAGTGTGCAAATAGT
CTACAAACCAGTTGACCTGAGCAAGGTGACCTCCAAGTGTGGCTCATTAGG
CAACATCCATCATAAACCAGGAGGTGGCCAGGTGGAAGTAAAATCTGAGAA

GCTGGACTTCAAGGACAGAGTCCAGTCGAAGATTGGGTCCCTGGACAATAT
CACCCACGTCCCTGGCGGAGGAAATAAAAAGATTGAA

7. Appendix B: Protein Purification

K18wt Ion Exchange Elution Profile:

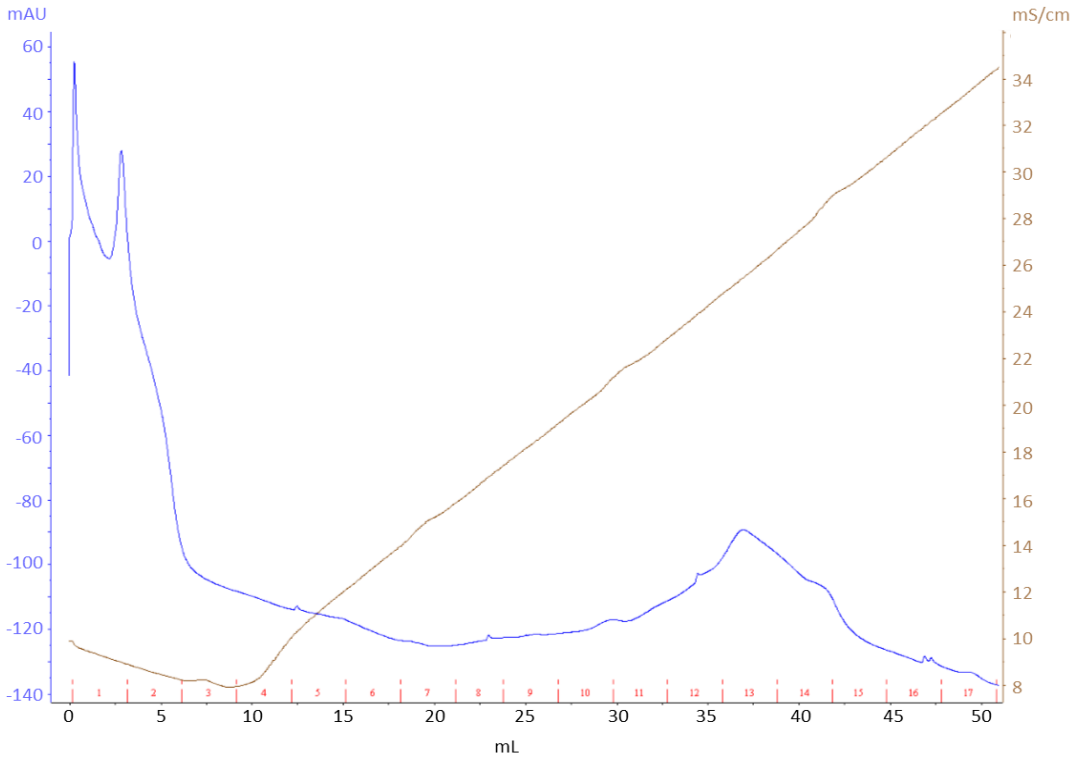

Elution profile of K18wt off the ion exchange column. The blue line denotes the UV abs at 280 nm. The brown line is the conductivity as the 1 M NaCl gradient is applied.

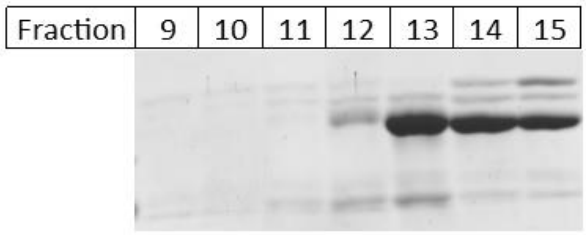

Fractions 9-15 of the trace above loaded onto a 15% polyacrylamide gel and resolved by SDS-PAGE to asses purity. Fractions 13-15 were pooled for size exclusion

K18wt Size Exclusion Elution Profile:

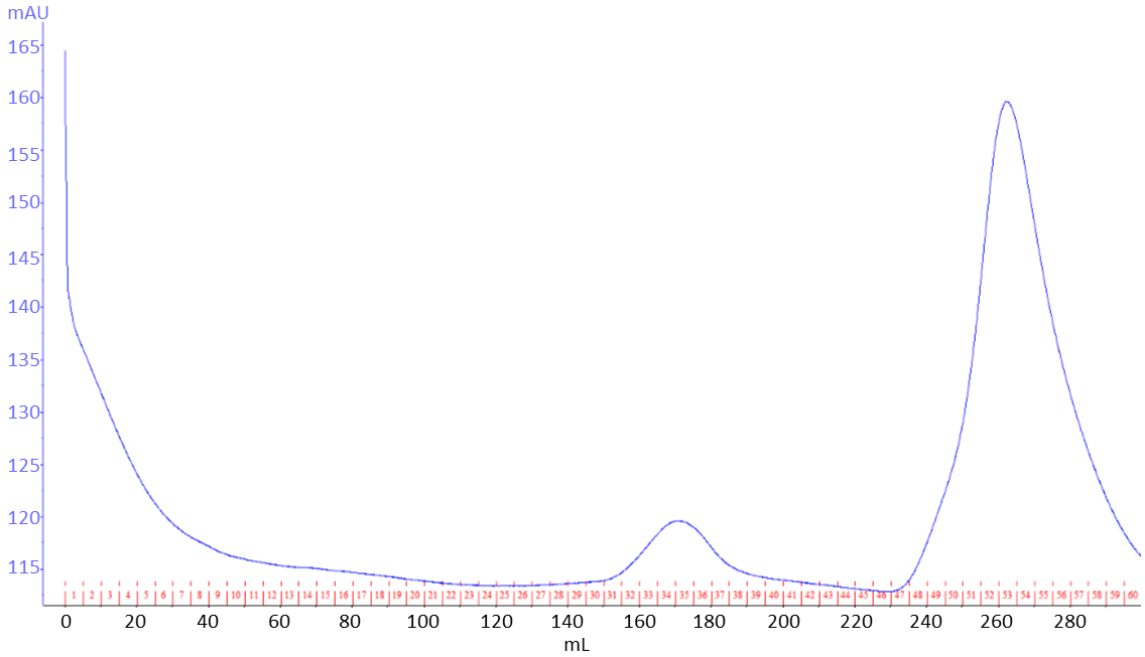

Elution profile of K18wt off the size exclusion column. The blue trace is the UV abs at 280 nm.

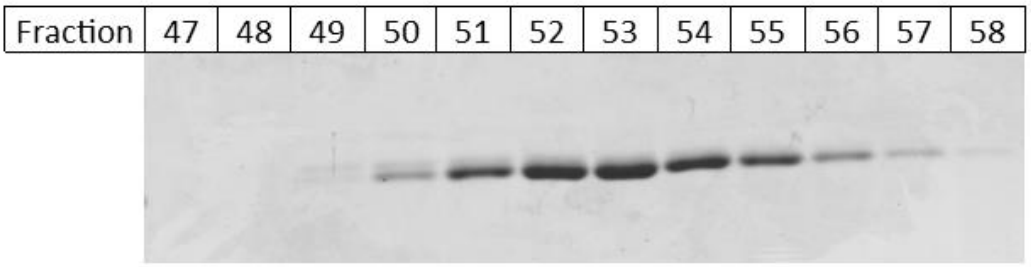

Fractions 47-58 were loaded onto a 15% polyacrylamide gel and resolved by SDS-PAGE to asses protein purity. Fractions 52-56 were pooled and precipitated to be monomerized.

8. Appendix C: MAP2 Inhibition Controls and K18P301S-YFP Puncta

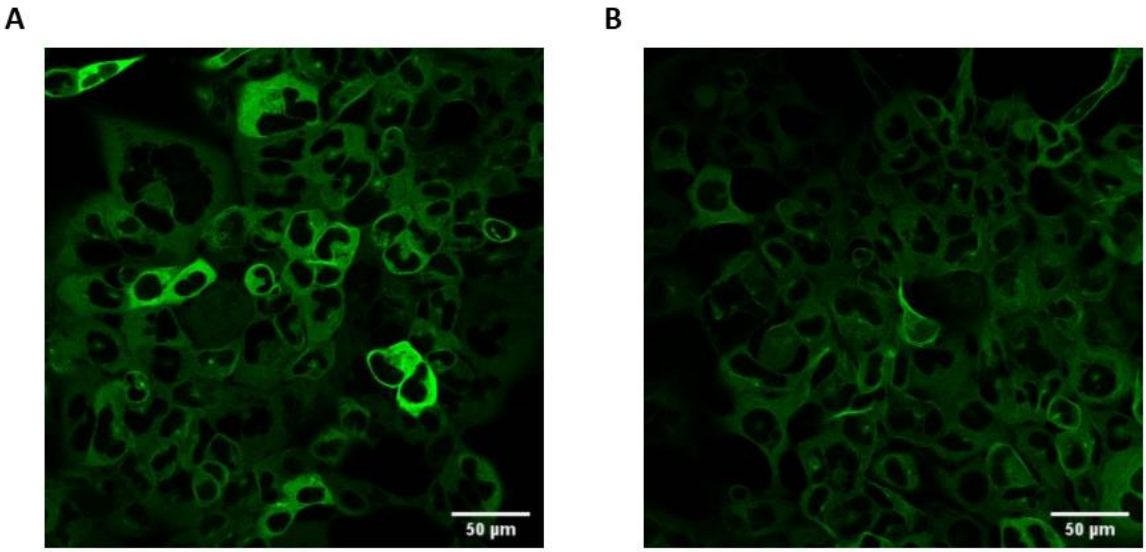

Tau Cells treated with 1 µM MAP2Ctr (A) or MAP2Dtr (B). Neither conditions show intracellular puncta formation.

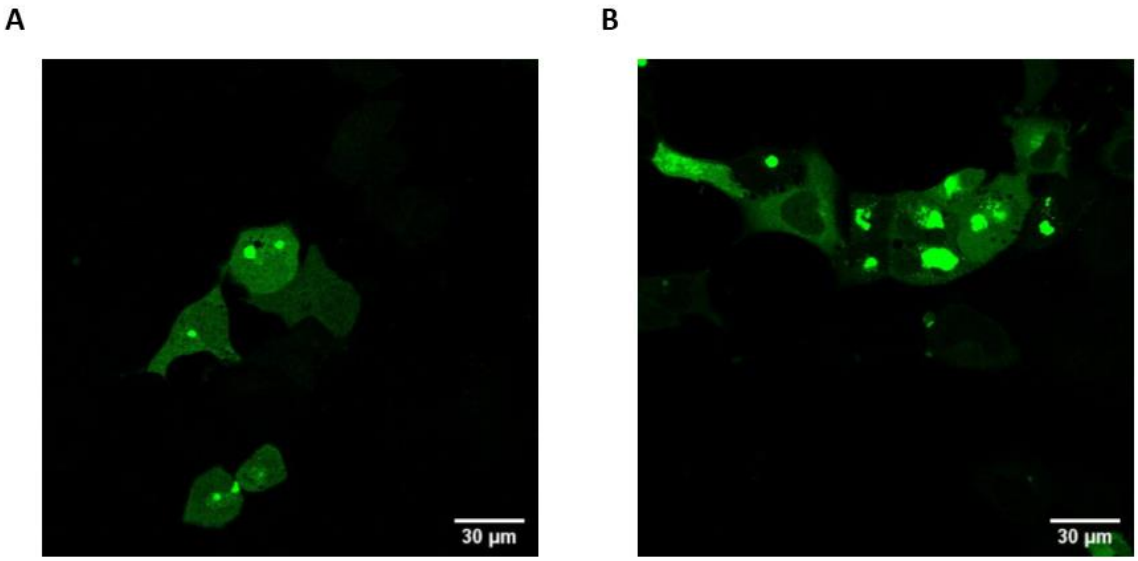

K18P301S-YFP cells transfected with 1 µM K18wt seeds. They form larger, more discrete puncta than the hT40P301S-YFP puncta.